Abstract

A new axial-flow wind air-turbine NU-102 having an external diameter of 1.2 m was developed in 1977 by the authors for harnessing the energy of high speed winds in Antarctica. This multi-blade wind-turbine is featured by the presence of a stator before the rotor, which enables the turbine to give a higher power, a higher torque at a lower rotational speed than an ordinary wind air-turbine. A 3-kW AC–DC generator is driven by the air-turbine through a planetary speed-up gear of speed ratio 6. The rotational speed of this generator can automatically be kept at a desired value even in violent blizzards by means of an electric eddy-current brake newly developed by the authors. The brake also affords a new means for converting the wind energy directly into heat through the liquid heated in the jacket of the brake-stator.

The present report describes the design of the whole system, the general performance of the air-turbine, and the combined performance of the wind-turbine and generator evaluated in wind-tunnel tests and field tests at Syowa Station. The field tests have proved that a generator output of 2.4 kW can be obtained at a wind velocity of 30 m/s, and that the rotational speed of the generator can be kept at a desired value for variable loads and wind velocities exceeding 30 m/s.

1. Introduction

In 1972, the authors designed and constructed a 2-kW wind air-turbine electric generator NU-101 (AWANO *et al.*, 1976), which was tested at Syowa Station by the 14th Japanese Antarctic Research Expedition (JARE–14). In 1977, another improved 3-kW wind air-turbine electric generator with an electric eddy-current brake was developed by the authors, which was designated as NU-102. This is now under field tests at Syowa Station by JARE–19. The present report describes the design details of NU-102 and its general performances as investigated by means of wind-tunnel experiments in Japan in 1977 and in field tests at Syowa Station in 1978.

The NU-102 is composed of an axial-flow multi-blade air-turbine with a stator similar to that of the NU-101, a planetary speed-up gear (speed ratio 6), an electric eddy-current brake, and a 3-kW AC–DC 24-V electric generator.

The stator has 45 stationary blades, and the rotor has 24 moving blades with an external diameter of 1.2 m. The boss-ratio is 1/3 and the annulus area is 1.005 m^2. The stator is placed before the rotor, and it deflects the inlet air from the axial direction towards the direction of rotation of the rotor by 39.9° at its outlet, so that the turbine speed may be lowered below that of the ordinary type with no stator. By virtue of this feature, the output turbine torque and power are greater than those of the ordinary type with the same diameter, and the NU-102 can withstand high wind speeds.

Another feature of the NU-102 is that it has an electric eddy-current brake for governing the rotational speed of the multi-blade air-turbine. The brake is consists of a brake-rotor having teeth and a brake-stator including a magnetizing coil and cooling jackets. By controlling the current flowing through the coil automatically, the rotational speed can be kept at a desired value even in violent blizzards. The energy absorbed by the brake is converted into heat by the electric eddy-current induced in the stator and on the teeth of the brake-rotor, and the resulting heat is transferred to the cooling liquid.

The electric brake can be used not only for governing the rotational speed, but also for converting the wind energy into heat which may be useful for heating rooms, melting ice, drying materials, and for other purposes, especially in Antarctica.

2. Details of the NU-102

2. 1. General feature of the NU-102

Fig. 1 shows the right side elevation, in longitudinal section, of the NU-102. Figs. 2 and 3 are photographs showing the inlet and outlet of the NU-102 in wind-tunnel tests respectively. The wind blows from right to left. The air-stream sur-

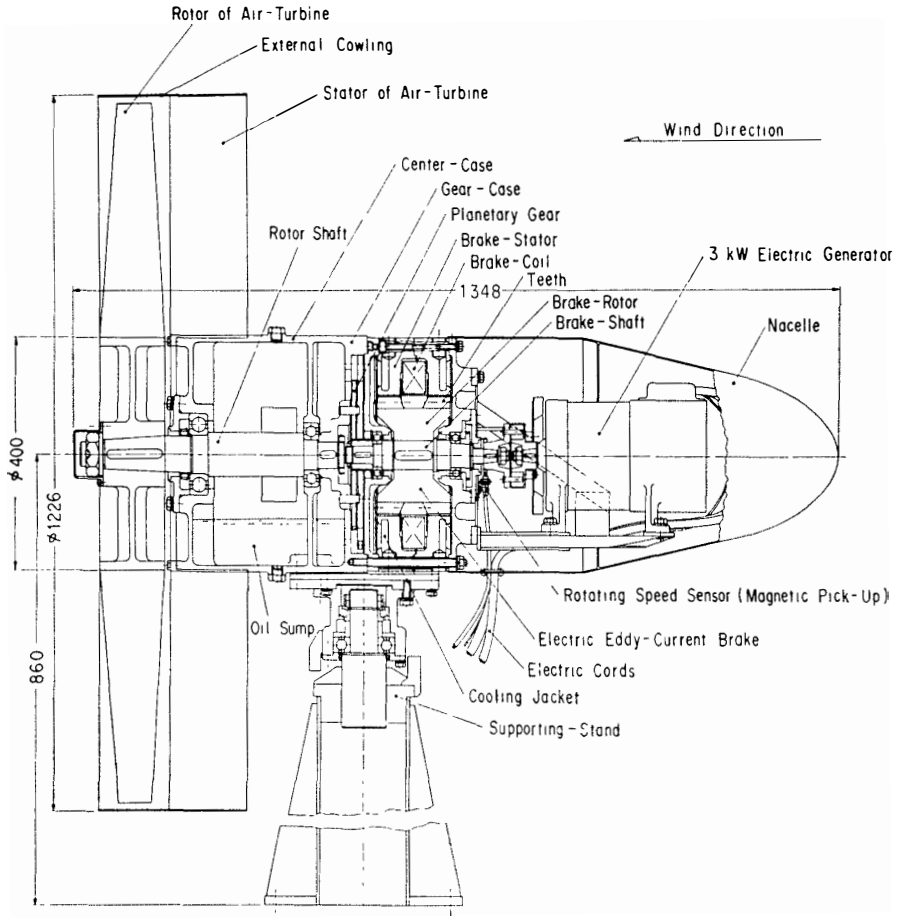

Fig. 1. Construction of the NU-102.

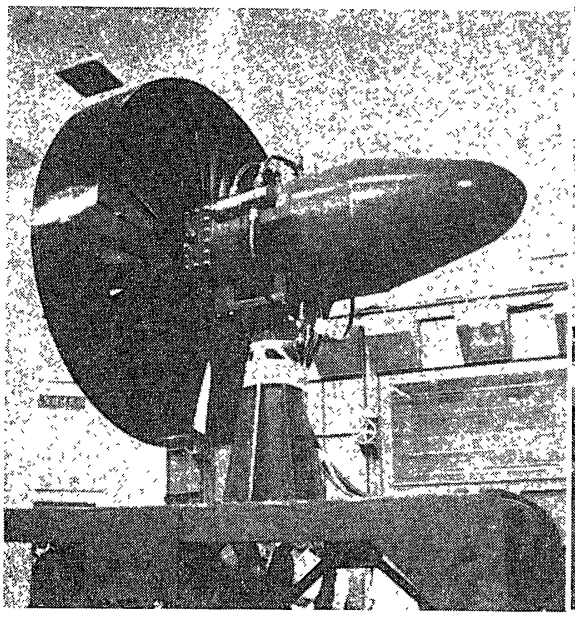

Fig. 2. The inlet side view of the NU-102.

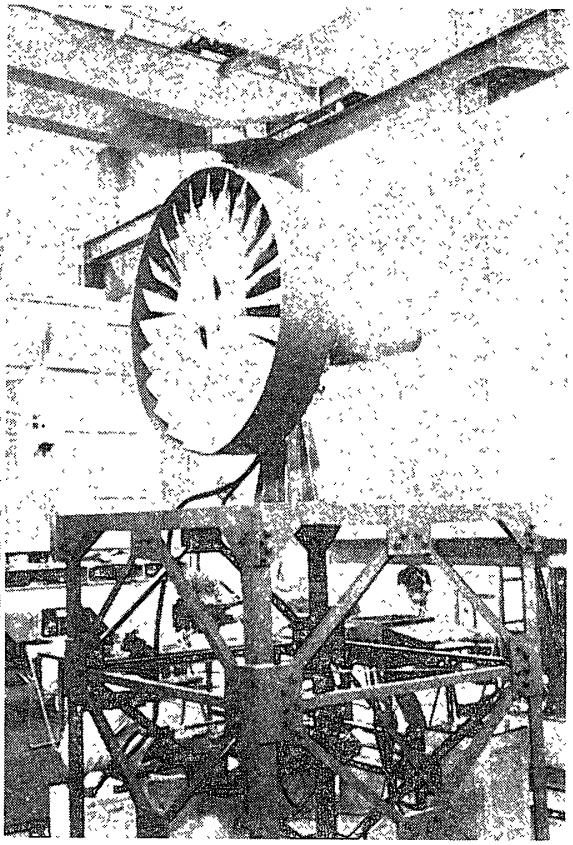

Fig. 3. The outlet side view of the NU-102 in wind-tunnel tests.

rounding the nacelle flows into the stator, which is composed of an external cowling of 1.226 m in diameter, 45 stationary blades, and an inner ring. The former two are made of stainless steel plates, and the ring is of a carbon steel pipe; these parts are welded to each other.

The air-flow is directed to a designed absolute velocity angle during it flows through the stationary blades. The outlet air from the stator flows into the rotor, which is provided with 24 moving blades, with designed relative velocity angles. The moving blades having a wing section and the boss are made of aluminium alloy; they are cast into an integral structure. The rotor shaft is supported by two ball bearings in a center-case of cast iron. The other end of the rotor shaft is coupled to a planetary speed-up gear. The gears and bearings are lubricated by splashing with the lubricant contained in the gear-case and the center-case.

Generally, the lubricant for the wind-mill should be low-viscosity oil, especially in cold districts. The lowest wind velocity required for starting an air-turbine depends mainly on the statical friction of the bearings and gears and on the moment of inertia of the rotating parts. The friction torque of the NU-102 is only 0.06 kg-m, and the air-turbine begins to rotate at a wind velocity as low as 1.4 m/s.

The output shaft of the planetary gear is coupled to the electric eddy-current brake. The brake-stator and the brake-rotor are made of pure iron providing high permeability for magnetic flux. The brake should be installed to the rear of the speed-up gear, because a smaller brake will suffice if its driving speed is higher. The other end of the brake shaft drives a 3-kW, AC–DC electric generator.

The output performance of a wind air-turbine electric generator depends in general on the efficiency of the air-turbine and generator, and on the matching characteristics of the generator to the air-turbine. However, we did not have time to develop a new electric generator matched to the air-turbine of the NU-102. We adopted a 3-kW, AC–DC electric generator for a marine diesel engine manufactured by Sawafuji Denki Co., Ltd., matching of which to the air-turbine was not very satisfactory. This is a separately excited AC three-phase generator, whose output is rectified to 24-V DC for charging batteries.

The rotational speed of the generator is detected by a magnetic pick-up and indicated on a speedometer on the controller panel. A small DC current is supplied from the batteries to the coil in the brake-stator, which brakes the brake-rotor. This current is regulated automatically so as to sustain a desired constant rotational speed even in violent blizzards. Thus the rotating parts of the NU-102 are protected from destruction.

2. 2. Wind air-turbine

The wind air-turbine is a multi-blade air-turbine having a stator before the rotor. In its external view, the NU-102 resembles a single row steam-turbine or

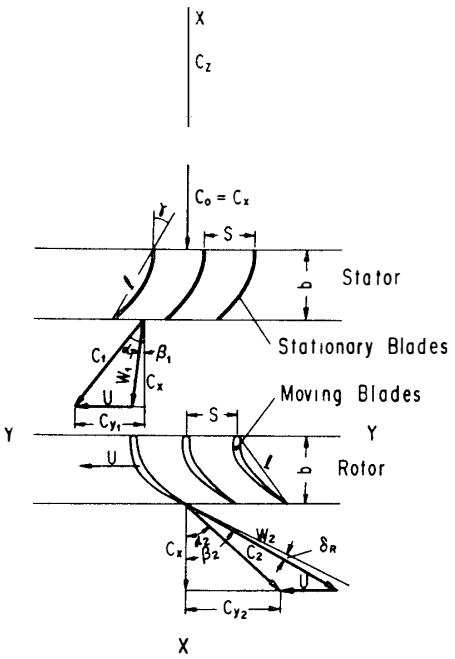

Fig. 4. Schematic arrangement of the stator and rotor.

gas-turbine. The schematic arrangement of stator and rotor and the velocity diagrams at the inlet and outlet of the rotor are shown in Fig. 4, in which the following notations are used:

C: absolute velocity, m/s,
W: relative velocity, m/s,
U: tangential velocity at a radius r, m/s,
XX: axis of the rotating shaft,
YY: tangential axis perpendicular to XX-axis,
α: angle between C and XX-axis, degree,
β: angle between W and XX-axis, degree,
γ: stagger angle, degree, or specific weight of air, kg/m^3,
ε: gas deflection angle, degree,
r: radius, m,
D: diameter, m,
H: blade height, $H=r_t-r_h$, m,
a: annulus area, $a=\pi(r_t^2-r_h^2)$, m^2,
G: weight flow rate of air, kg/s,
l: chord length, m,
b: axial chord length, m,
S: spacing of blades, m,
T_t: turbine torque, kg·m,
T_g: generator torque, kg·m,
T_f: friction torque, kg·m,
L_{ti}: indicated output of the air-turbine, kW,
L_{te}: brake output of the air-turbine, kW,
L_g: generator output, kW,
η_{TT}: total-to-total efficiency of the air-turbine,
η_{TS}: total-to-static efficiency of the air-turbine,
η_g: generator efficiency,
g: gravity acceleration, $g=9.8$ m/s^2,
P: static pressure, mmHg abs.,
t: static temperature, °C.

Subscripts z: indicates the quantities measured at a point on the XX-axis sufficiently distant from the stator,
0: indicates the quantities measured just ahead of the stator,
1: indicates the quantities measured at the exit of the stator,
2: indicates the quantities measured at the exit of the rotor,
s: indicates the stationary blade,
R: indicates the moving blade,
g: indicates the generator,
t: indicates the quantities measured at the tip radius, or indicates the

turbine,
m: indicates the quantities measured at mean radius,
h: indicates the quantities measured at hub radius,
i: indicates quantities, not including mechanical losses,
th: theoretically calculated quantities,
D: dynamometer test results,
$*$: indicates the values at a designed point,
c: indicates the values at the nominal state,
max: indicates the maximum values.

The stator has been designed according to the principle of "constant nozzle angle design": the exit angle from the stator is kept constant for any radius, the rotor is of an "axially leaving velocity design": the absolute exit velocity C_2 from the rotor is directed axially at any radius in the design point. Further details are shown in the Appendix and references (AWANO *et al.*, 1976).

The stationary blade has no wing section but has a parabolic camber line. The moving blade of the rotor has a wing section of T-6 (HORLOCK, 1966) with a parabolic camber line. The rotor was balanced statically after the boss had been machined and fixed to the shaft. The maximum rotational speed of the NU-102 does not exceed 1000 rpm; accordingly, the tensile stress due to centrifugal force and the bending stress acting on the root of the moving blades are very low, which enabled us to fabricate the rotor by aluminium casting.

2. 3. Speed-up gear

In designing an air-turbine generator, attention has to be paid to the speed-up gear. A planetary gear is most suitable for the wind air-turbine, in that it affords high speed ratios and low mechanical losses, and in that its output shaft can be coaxially alined with the input shaft. It is expensive, though.

We developed a very compact planetary gear with a speed ratio of 6 with the aid of Toyo Seimitsu Zoki Co., Ltd., which is shown in Fig. 5. A disk is attached to the end of the output shaft of the air-turbine, which holds three planetary gears with 50 teeth of module 2. These gears roll along the inside of a fixed internal gear with 125 teeth and drive a sun gear with 25 teeth, which drives the brake-rotor.

The speed ratio of such system is represented by

$$N_g/N_t=1+(Z_f/Z_s)=1+(D_f/D_s) \tag{1}$$

where N_g: rotational speed of the generator, rpm,
N_t: rotational speed of the air-turbine, rpm,
Z_f: number of teeth of the fixed gear,
Z_s: number of teeth of the sun gear,
D_f: pitch circle diameter of the fixed gear, mm,
D_s: pitch circle diameter of the sun gear, mm.

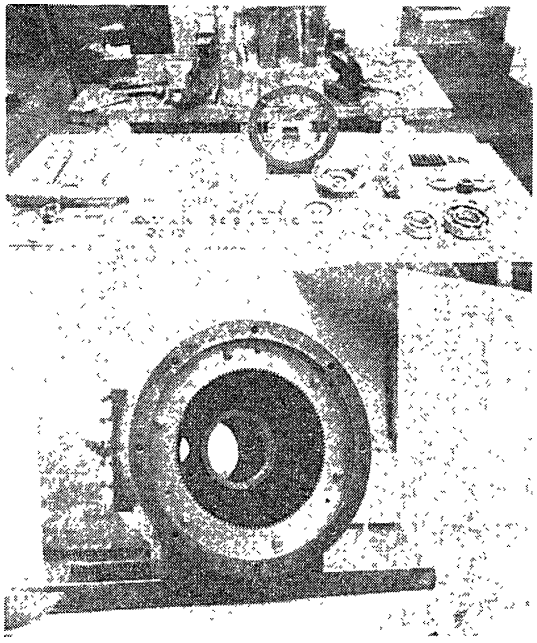

Fig. 5. Planetary speed-up gear for the NU-102 (speed ratio 6).

The boss-ratio and accordingly, the internal diameter of the air-turbine should be so determined that the fixed gear can be held. In the NU-102, $Z_f=125$, $Z_s=25$ and $D_f=250$ mm, $D_s=50$ mm. Hence the speed ratio is 6.

The disk and gear are installed in a very narrow gear-case attached to the center-case, and the two cases are connected to each other by a bottom hole and filled with lubricant.

2. 4. Electric eddy-current brake

As stated before, a new speed controlling system has been developed for protecting the multi-blade air-turbine from violent blizzards. The principle of the electric brake we adopted for this purpose is shown in Fig. 6. The details are shown in Fig. 7. The electric brake is composed of a brake-rotor and a brake-stator. The brake-rotor, made of pure iron, is supported by two ball bearings and has 30 teeth cut on its circumference and it has an external diameter of 200 mm. The brake-stator, also made of pure iron, consists of two symmetric pieces. They

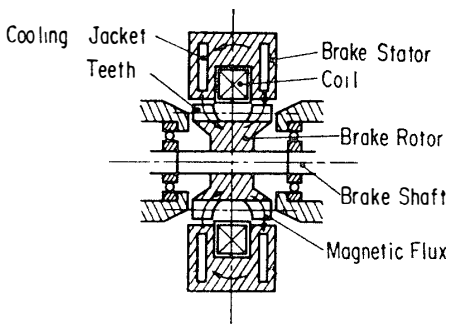

Fig. 6. The principle of the electric eddy-current brake for the NU-102.

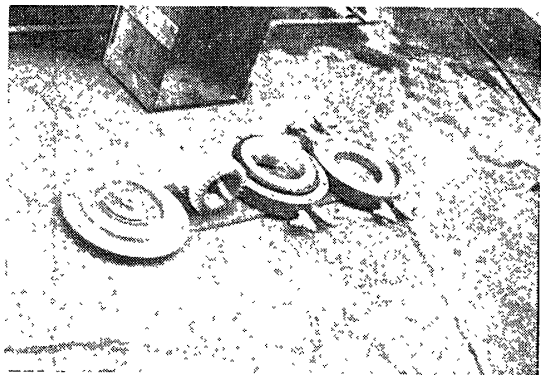

Fig. 7. The electric eddy-current brake for the NU-102.

were fixed together by bolts after a ring-shaped magnetizing coil had been inserted between them so as to surround the shaft. The brake-stator, provided with cooling jackets, surrounds the brake-rotor with a very narrow gap between the two. The magnetizing electric current is supplied to the coil from 24-V batteries and is controlled by an electric controller (Fig. 8). The electric circuits of the controller are shown in Figs. 9 and 10. When a small current is supplied to the coil, a ring-shaped magnetic flux is formed around the coil through the brake-stator and brake-rotor. The rotor teeth cut the magnetic flux, and the brake-stator and the teeth are heated by the induced electric eddy-current. The rotor is braked by the resisting torque, and the speed is reduced. By automatically regulating the coil current, a constant rotational speed can be maintained independently of variation in the input power and in the load.

The heat generated in the brake-stator is transferred to the cooling liquid in the jackets. This is to be dissipated somehow in order to keep the stator coil temperature within the allowable range. In the NU-102, two small tube-type radiators are provided for dissipating the heat into the Antarctic cold atmosphere. The natural convection caused by the temperature difference in the heated liquid is utilized for recirculating the liquid between the radiators and the jackets.

The electric eddy-current brake gives us not only a new means of speed govern-

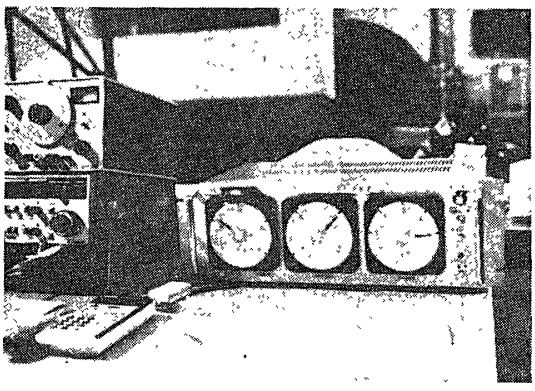

Fig. 8. Electronic speed controller for the NU-102.

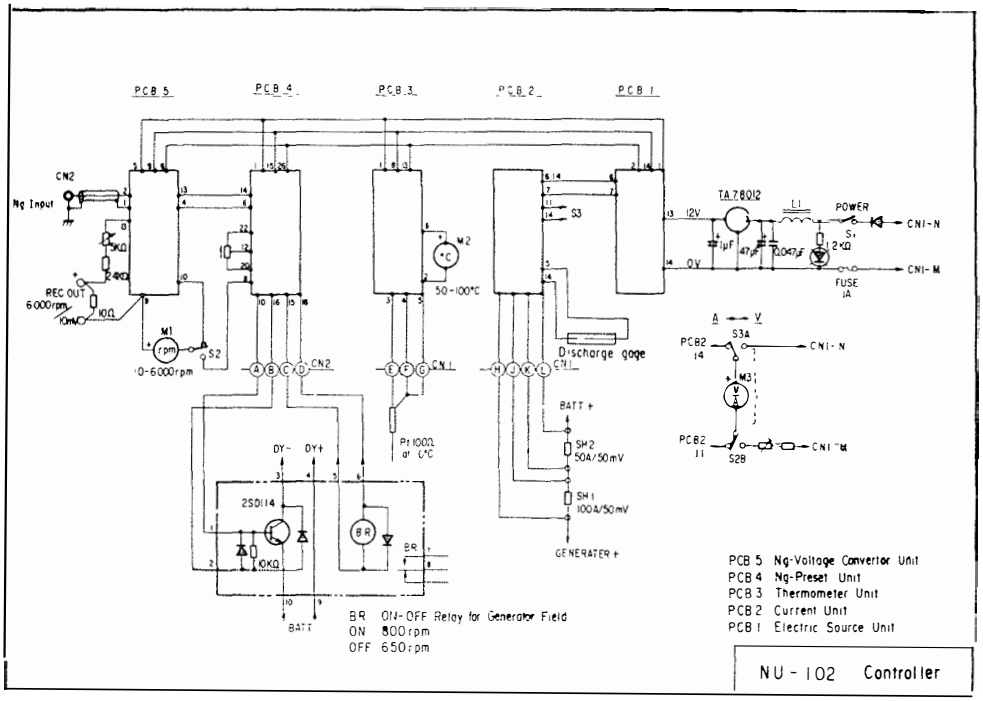

Fig. 9. The electrical circuits of the speed controller for the electric eddy-current brake.

ing of wind air-turbine but also a way of converting the output of the air-turbine into heat directly. If desired, the heated liquid may be utilized for heating rooms, for melting ice, and for many other purposes by circulating it through a small pump driven by the wind-mill or by another small electric motor.

The automatic rotational speed controller we developed for the NU-102 is shown in Fig. 8. The following three meters are arranged on the panel from left to right: an ammeter/voltmeter for measuring the generator output (0–120A/0–40V DC), a thermometer indicating the maximum liquid temperature in the jacket (t_w= −50–100°C), and a rotational speedometer for the electric generator (N_g=0–6000 rpm). On the right end of the panel, the following are arranged in a line from top to bottom.

(a) A selective switch for A/V,
(b) A dial for pre-setting an arbitrary braking rotational speed N_q,
(c) A push button for checking the pre-set braking rotational speed (The braking speed pre-set by (b) is indicated on the rotational speedometer by pushing this button),
(d) An on-off indicating lamp for the electric source,
(e) An on-off switch for the electric source, 24-V.

An allowable maximum rotational speed of the generator is to be pre-set by (b), and checked by (c). The controller contains also an automatic switching circuit for the field current of the generator. The current is switched on if the generator speed

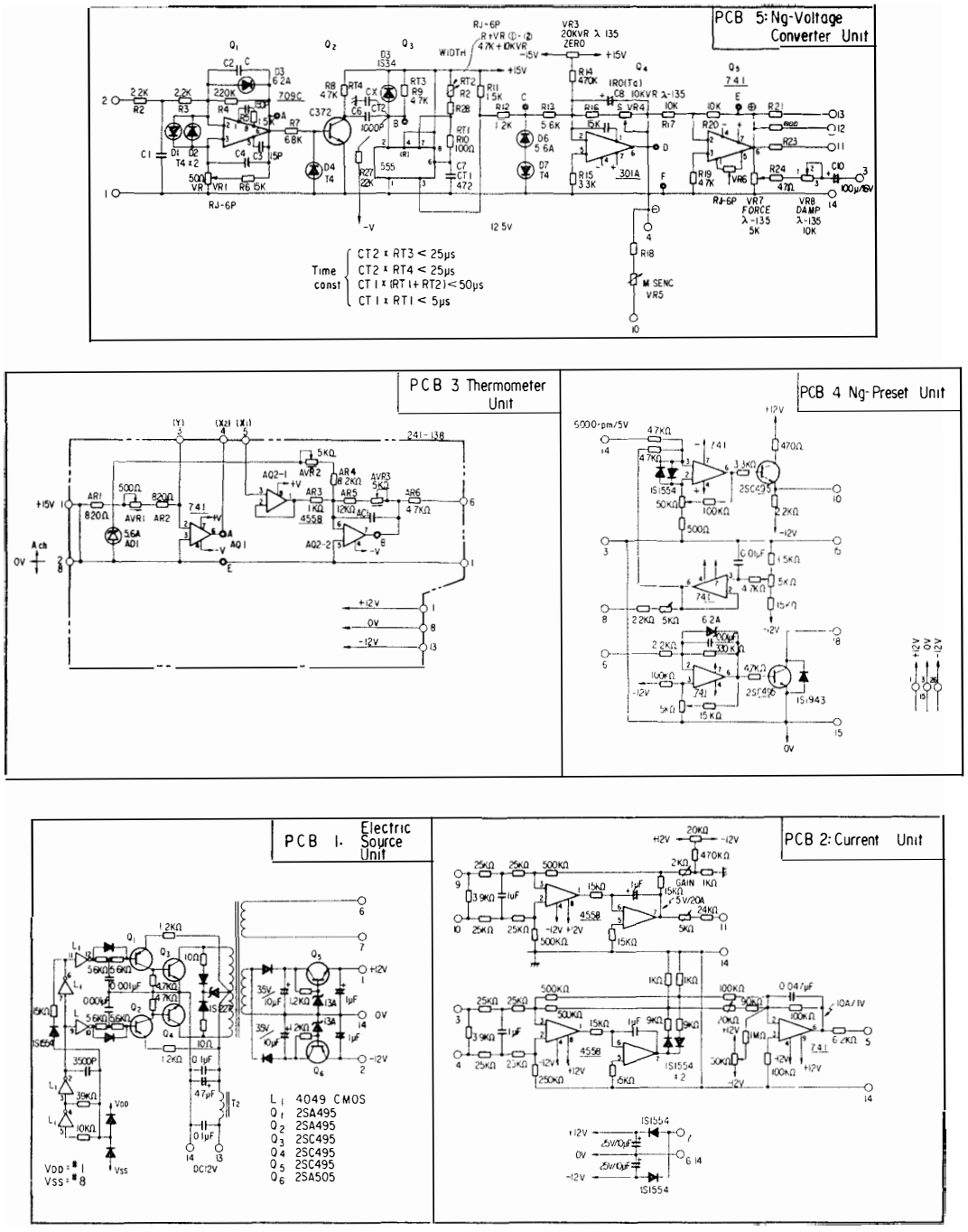

Fig. 10. Electrical connection diagrams of the speed controller for the electric eddy-current brake.

N_g reaches 600 rpm.

When N_g reaches the pre-set braking speed, a small current begins to flow through the magnetizing coil; the pre-set speed can be maintained by increasing the

current automatically with the increase in wind velocity. By this means, a desired maximum rotating speed of the generator, or of the air-turbine, can easily be maintained in violent blizzards.

If the braking current is cut off, all of the output of the air-turbine has to be absorbed only by the electric generator. On the contrary, if the electric generator is kept in a no-load state, all the output has to be absorbed only by the electric brake.

2. 5. Installing the NU-102 in the field

The wind electric generator NU-102 was mounted on a base plate of a framework rack with a height of 1.9 m for preventing it from being buried in deep snow, for preventing breakage of the moving blades due to sucked-up foreign matter, and for ensuring the safety of personnel.

With an ordinary wind-mill, mounting the wind-mill on a high tower or a rack would be a hard task especially in very cold places such as Antarctica. This is not the case with the NU-102, which is very small: it can well be transported by a helicopter from the ship FUJI to Syowa Station. After being rebuilt in a warm room, it can be mounted on a rack in the field or transported to another spot by a sleigh.

A connection box and 24-V batteries should be installed as near to the wind-mill as possible for preventing voltage drop in the electric cords, in which currents up to 120 A will flow. The automatic controller may be set in a warm room far from the wind-mill.

The battery room should be well ventilated, because hydrogen may be generated if the batteries are overcharged.

The NU-102 has no tail wing that is usually employed as a direction stabilizer, but the stator and rotor themselves act as a rudder and they are always leeward. This direction-stabilizing effect was verified by the wind-tunnel tests in Tokyo and also by field tests in Antarctica by JARE–19. Such tailless air-turbine is simple and inexpensive, but some aerodynamical losses are unavoidable.

The NU-102 has no slip ring in the electric output circuit. For ensuring the free rotation of nacelle around the axis of the supporting stand, two cables connecting the electric generator to the batteries are placed loosely around the support. Difficulties due to slip rings can completely be eliminated by this simple method.

The body and the nacelle containing the speed-up gear, the electric brake and the generator are supported by a taper roller bearing and a ball bearing on top of the supporting stand. The bearings are lubricated by antarctic grease.

2. 6. Electric generator

As stated before, a 3-kW, AC–DC generator made by Sawafuji Denki Co., Ltd. is used for the NU-102, although its performance is not well matched to our

air-turbine. The details of the generator are shown in the Appendix. Its output performance at full load and partial loads are given in Fig. 11.

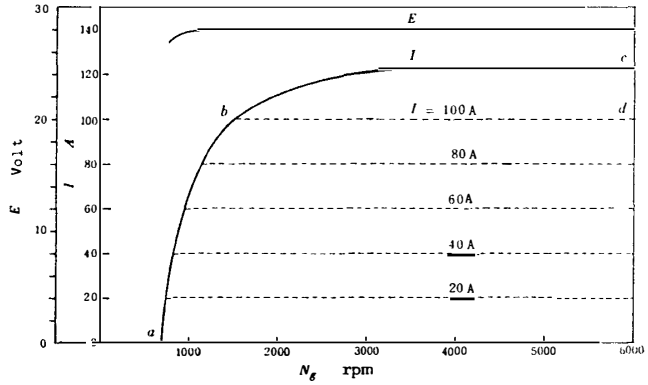

Fig. 11. Full load and partial load performances of the Sawafuji 3-kW, AC–DC electric generator for charging 24-V batteries.

3. Output Performance of the Air-Turbine NU-102

The output performance of the air-turbine NU-102 was measured in the wind-tunnel built in 1976 at Narashino Campus of the College of Science and Technology of Nihon University. It has an exit opening of 2 m×2 m; the maximum wind velocity is 50 m/s. The nacelle cowling and the generator of the NU-102 were removed, and an electric eddy-current dynamometer was substituted in place of the latter. The torque absorbed by the dynamometer was measured by an electric load-cell shown in Fig. 12.

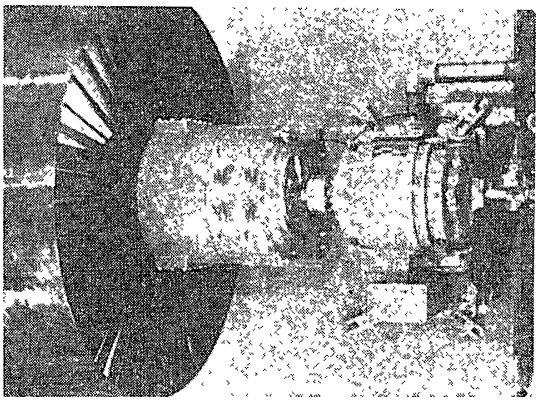

Fig. 12. Electric dynamometer tests of the NU-102 (from above).

3. 1. Experiments on the effect of the number of stationary blades

We made a series of experiments on the effect of the number of stationary blades and of their solidity on the performance of the air-turbine. Two stators were prepared for this purpose. One had 30 blades and the other 45 blades. Fig. 13 shows the torque developed by each stator. Under a constant wind velocity C_z, the turbine torque T_t decreases with the increase in turbine speed N_t. The maximum turbine speed, which is obtained at no-load, *i.e.*, at $T_t=0$, is not affected by the number of stationary blade. However, if the number of blades is increased the turbine torque at low turbine speeds is increased and, accordingly, the slope $(\partial T_t/\partial N_t)$ is increased.

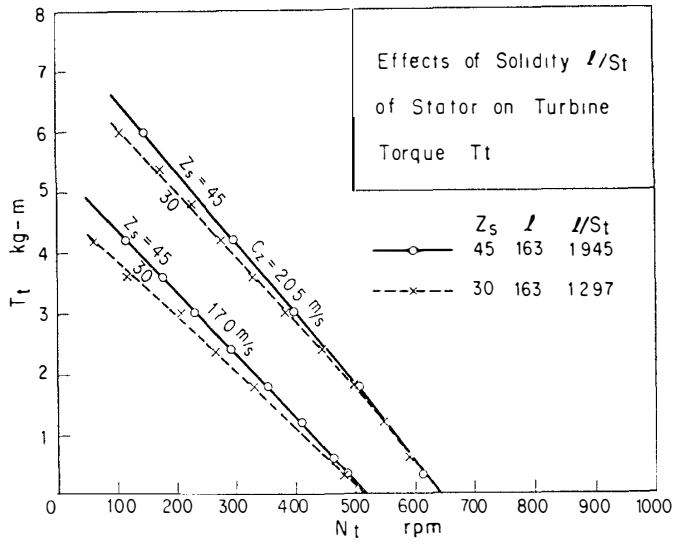

Fig. 13. Turbine torque, T_t vs. turbine speed N_t. The effects of the number of stationary blades.

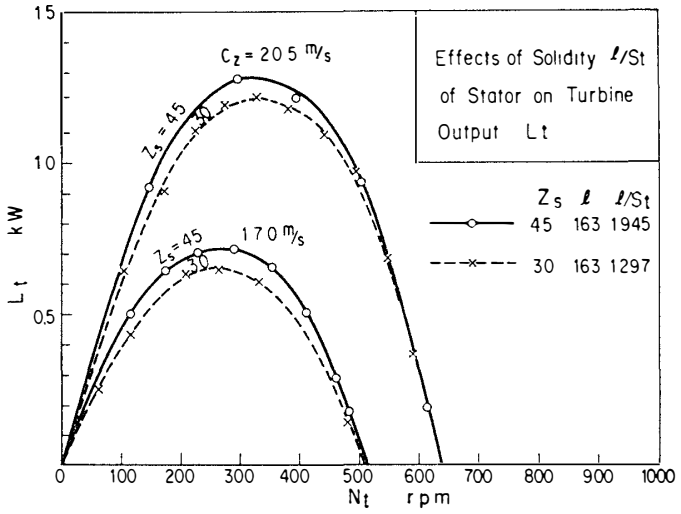

Fig. 14. The effects of the number of stationary blades on the turbine output power L_t, N_t represents the turbine speed.

Fig. 14 shows the effects of the number of stationary blades on the output power L_t. The maximum turbine output is increased from 1.22 kW to 1.28 kW at C_z=20.5 m/s if the number of the stationary blades is increased from 30 to 45. The solidity l/S_t of the stationary blades at tip radius was 1.297 and 1.945 for 30 and 45 blades, respectively. The experimental results show that a solidity value slightly higher than that usual with steam and gas-turbine is to be recommended for an air-turbine with stator. In practice, the number of stationary blades should be determined considering economy, weight, and performance. We adopted a turbine

with 45 stationary blades because its output can be 4.9% higher than a 30 blade turbine.

3. 2. Turbine torque and maximum speed

The relation between the turbine torque T_t and the turbine speed N_t as obtained by dynamometer tests is shown in Fig. 15. The tests were carried out for wind velocities from 10.0 m/s to 33.7 m/s under various loads. The turbine speed N_t at a constant wind velocity C_z increases linearly with the decrease in torque T_t and reaches a maximum $(N_t)_{max}$ at no-load or $T_t=0$. The negative slope, $(\partial T_t/\partial N_t)$, increases with the increase in wind velocity.

As shown in Fig. 12, the inlet annulus area is partly in the shade of the dynamometer. Accordingly, the values of torque T_t and output L_t obtained by the dynamometer rests may be slightly lower than those expected under the working conditions, in which the generator is completely enclosed in the nacelle.

The air-turbine started to rotate at a wind velocity as low as 2.0 m/s in the dynamometer tests, and 1.4 m/s in the field tests of the completed NU-102.

The torque developed by an air-turbine can in general be represented by

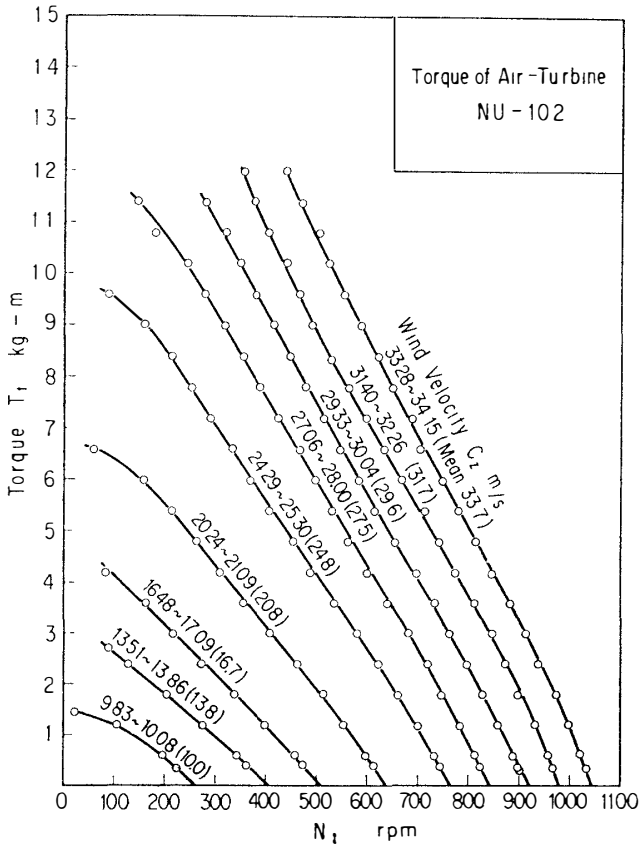

Fig. 15. The turbine torque of the NU-102.

$$T_t=a-bN_t \quad \text{kg·m} \tag{2}$$

where

$$a=k_1C_z^2,$$
$$b=k_2C_z, \tag{3}$$

and k_1 and k_2 are constants determined by the design of the air-turbine. For the NU-102,

$$k_1=0.0185 \quad \text{and} \quad k_2=0.00061. \tag{3'}$$

The maximum rotational speed of an air-turbine at no-load can be obtained by putting $T_t=0$ in eq. (2):

$$(N_t)_{max}=a/b=(k_1/k_2)C_z \quad \text{rpm.} \tag{4}$$

For the NU-102,

$$(N_t)_{max}=30.3C_z \quad \text{rpm.} \tag{4'}$$

3.3. Turbine output and optimum turbine speed

If T_t is given by eq. (2), the output power L_t for a speed N_t can be calculated as follows:

$$L_t=2\pi N_tT_t/6120=0.001027N_tT_t$$
$$=0.001027(aN_t-bN_t^2) \quad \text{kW.} \tag{5}$$

Eq. (5) shows that the output power should be given by a parabola, if plotted against N_t, see Fig. 16. The maximum power is obtained at the optimum speed $(N_t)_c$ for which

$$\partial L_t/\partial N_t=0. \tag{6}$$

From eqs. (5) and (6), we can show that, for a given wind velocity C_z,

$$(N_t)_c=a/2b=(N_t)_{max}/2. \tag{7}$$

This equation, which shows that the optimum speed giving the maximum output power $(L_t)_{max}$ is one half of the maximum turbine speed $(N_t)_{max}$ to be obtained at no-load under the same wind velocity, should be remembered in the design of an air-turbine.

By substituting eq. (7) into eq. (5), we obtain

$$(L_t)_{max}=0.001027(a^2/4b)$$
$$=0.0002568(a^2/b)$$
$$=0.0002568(k_1^2/k_2)C_z^3 \quad \text{kW.} \tag{8}$$

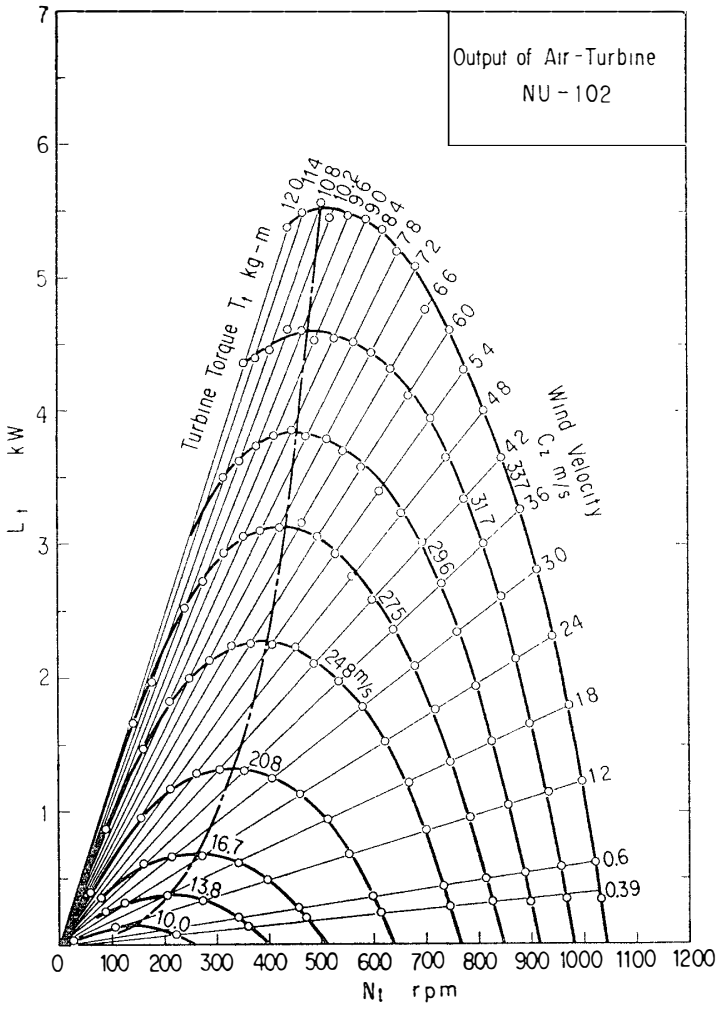

Fig. 16. Turbine output power of the NU-102 measured by dynamometer tests.

For the NU-102,

$$(L_t)_{max}=0.000144C_z^3 \quad \text{kW}. \tag{8'}$$

The results calculated with these experimental formulae are shown in Table 1 for wind velocities less than 60 m/s.

Table 1. The maximum turbine speed $(N_t)_{max}$ and the maximum turbine output power $(L_t)_{max}$ at the optimum turbine speed $(N_t)_c$ for different values of wind velocity C_z. Q_H is the maximum heat generated in the electric brake.

Wind velocity C_z m/s	$(N_t)_{max}$ rpm	$(N_t)_c$ rpm	$(L_t)_{max}$ kW	Q_H kcal/h
0	0	0	0	0
5	152	76	0.018	15
10	303	152	0.144	124
15	455	228	0.486	418
20	606	303	1.15	989
25	758	379	2.25	1,935
30	909	455	3.89	3,345
35	1060	530	6.17	5,310
40	1212	606	9.22	7,930
45	1364	682	13.1	11,270
50	1515	758	18.0	15,500
55	1667	834	24.0	20,600
60	1818	909	31.1	26,750

4. Combined Performance of the NU-102 with Electric Generator under Loads

Some wind-tunnel tests were carried out to study the combined performance of the NU-102 and the 3-kW electric generator. A 24-V battery and six Ni–Cr wires, each with 1 ohm resistance, were connected to the generator as shown in Fig. 17. The tests were carried out under a no-braking condition, *i.e.* with no magnetizing current in the eddy-current brake.

a. The generator is charging a battery and supplying a current I_A to the resistance R_A (under a light load).

b. The generator and a battery are supplying a current I_A to the resistance R_A (under a high load).

Fig. 17. Load circuits of the generator.

Figs. 18, 19 and 20 show the output voltage E, the output current I, and the output power of the generator L_g, as functions of the turbine speed N_t and generator speed $N_g(=6N_t)$. Since the generator had been designed for marine diesel engines, it gave no voltage output until the speed reached about 600 rpm. When the generator speed rose to 600 rpm, output rose steeply to 25-V, to start charging the battery.

In these figures, B denotes the battery (24-V, 120 A). The notation $(B+1/3)$ indicates that the battery and three Ni–Cr wires are connected in parallel so that the resistance of the latter is 1/3 ohm. Fig. 20 shows that the maximum load that can be given to the NU-102 is about $(B+1/3)$, because the minimum voltage required for charging the battery, 25 V cannot be maintained for larger loads. The NU-102 begins charging the battery at a wind velocity of 10.3 m/s. The generator speed increases with the increase in wind velocity and reaches the maximum allowable speed of 6000 rpm at a wind velocity of 30–32 m/s under verious loads (Fig. 18). This shows that the maximum allowable wind velocity for the NU-102

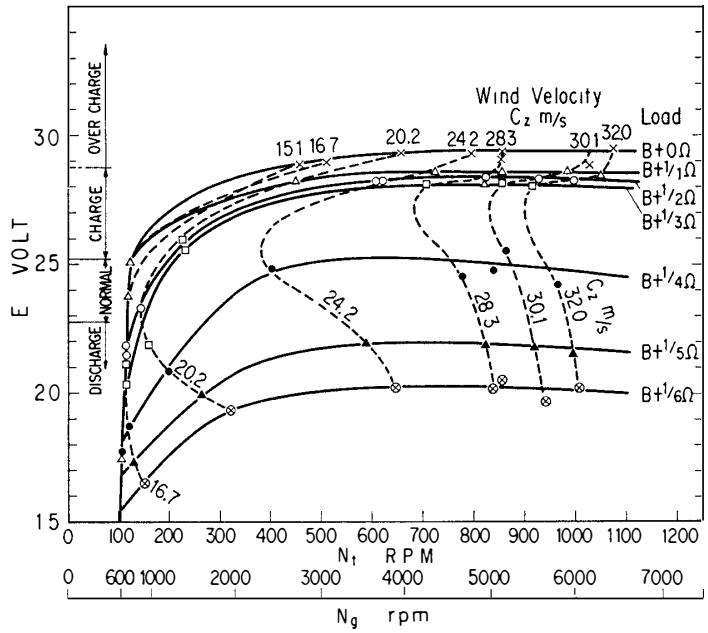

Fig. 18. The output voltage E of the generator vs. turbine speed N_t and wind velocity C_z under various loads.

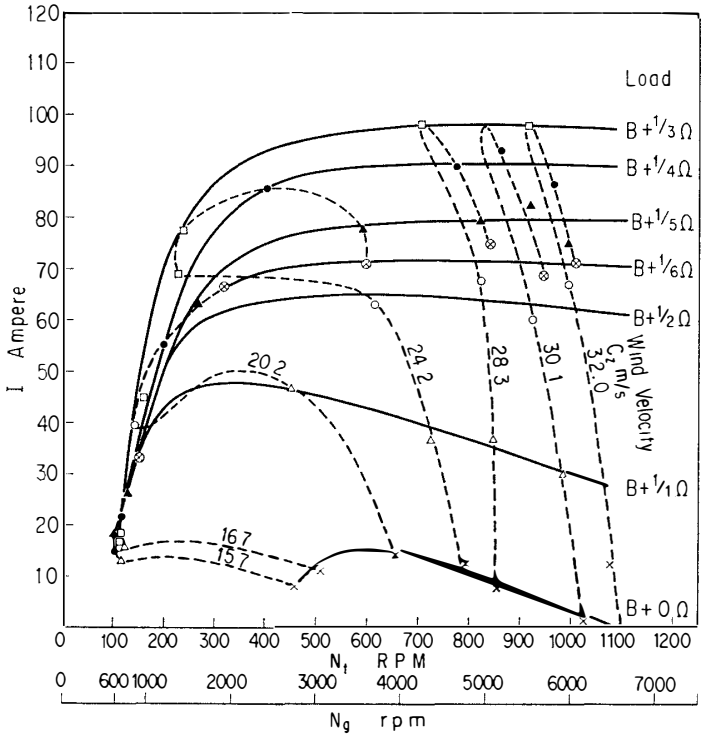

Fig. 19. The output current I of the generator vs. turbine speed N_t and wind velocity C_z under various loads.

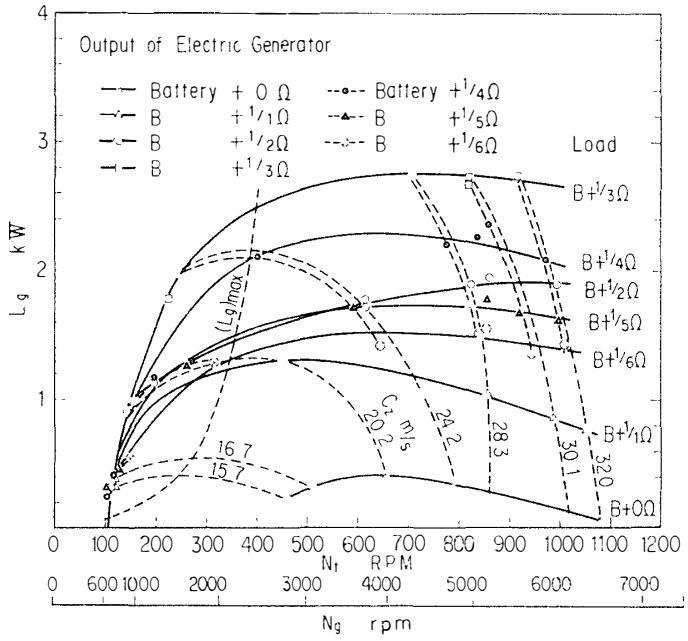

Fig. 20. The output power L_g of the generator for any turbine speed N_t and wind velocity C_z under various loads.

is 30–32 m/s if the electric brake is not used. Under a light load, apart of the current I charges the battery, the rest of the current being dissipated in the resistors (see Fig. 17a). Under heavy loads over $(B+1/3)$, the output voltage is decreased to normal or discharging voltages as shown in Fig. 18: the discharging current from the battery flows through the resistors, and the output current from the generator, I, is decreased as shown in Fig. 17b. If I, I_A, and I_B represent the generator output current, the current flowing through the resistors R_A, and the current flowing into or out of the battery with an internal resistance R_B, respectively, then in charging the battery,

$$I=I_A+I_B=E(1/R_A+1/R_B)=E/R; \tag{9}$$

and in discharging the battery,

$$I=I_A-I_B=E(1/R_A-1/R_B)=E/R. \tag{10}$$

Table 2 gives the values calculated with eqs. (9) and (10) as compared with the experimental results. In charging, R_B remains constant when R_A is varied. In discharging, R_B decreases with the increase in I_B, and the total resistance R remains almost constant.

Fig. 20 shows the output power of the generator calculated as

$$L_g=EI/1000 \quad \text{kW}. \tag{11}$$

At a constant speed, the output increases with the increase in load, reaches a maximum at a load equal to $(B+1/3)$, and decreases again if the load is further

Table 2. The output current of the generator I in charging or discharging the battery (see Fig. 17).

	x	R_A Ω (meas.)	E V (meas.)	I_A A (calc.)	I_B A (calc.)	$I=I_A \pm I_B$ A (calc.)	I A (meas.)	R_B Ω	R Ω
In charging battery	1	1.02	28.5	27.7	9.5	37.2	30–45	3	0.768
	2	0.51	28.4	55.7	9.5	65.2	62–65	3	0.436
	3	0.34	28.1	82.7	9.4	92.1	95–98	3	0.306
In discharging battery	4	0.25	24.5	98	9.8	88.2	90	2.5	0.278
	5	0.20	21.8	109	30.7	78.3	78	0.71	0.279
	6	0.17	20.0	118	47.6	72.4	72	0.42	0.276

Remarks x: number of Ni-Cr electric resistance wires connected in parallel to a 24-V battery
meas.: measured
calc.: calculated

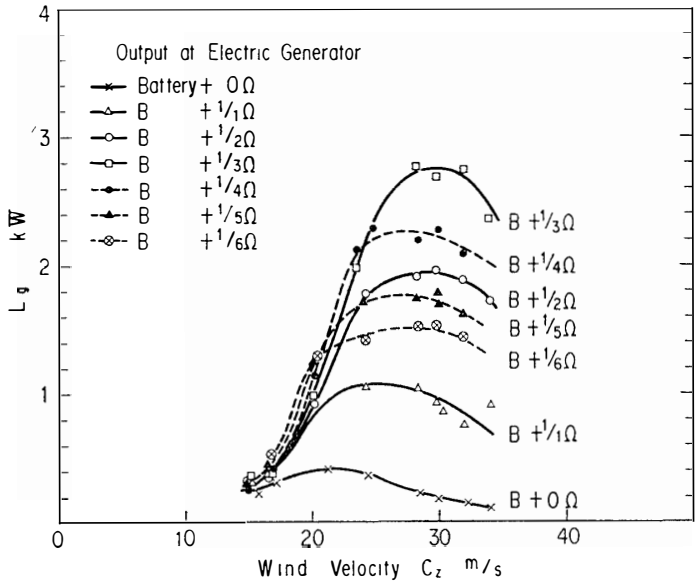

Fig. 21. The output power of the generator L_g for any wind velocity C_z under various loads.

increased. Fig. 21 shows the generator output L_g of the NU-102 against the wind velocity for various loads. The maximum power, 2.8 kW, is obtained at a wind velocity of 30 m/s and for a load (B+1/3).

If the turbine output L_t at a wind velocity C_z is greater than the maximum generator output under a certain load, the output of the system is determined by the latter and not by the former.

The efficiency η_g of the 3-kW electric generator has been determined by dynamometer tests and is estimated at about 73%.

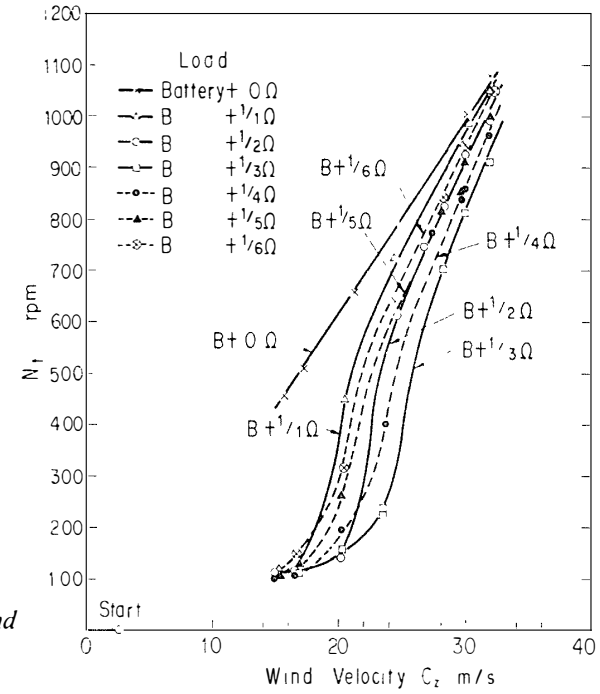

Fig. 22. The turbine speed N_t for any wind velocity C_z under various loads.

Fig. 22 shows the rotational speed of the air-turbine N_t against the wind velocity C_z for various loads. The N_t vs. C_z relation is not linear and varies remarkably with the load. At wind velocities below 26 m/s, N_t for $(B+1/3)$ is lower than the designed value of optimum turbine speed $(N_t)_c$ for the wind velocity C_z. At wind velocities over 26 m/s, it is higher than the designed value of $(N_t)_c$ (see Fig. 24).

5. Torque Matching between Air-Turbine and Generator

Fig. 11 shows the general output characteristics of the 3-kW generator. The output voltage E rises to about 28-V when the generator speed N_g reaches 600 rpm, and the voltage is maintained constant up to 6000 rpm. The generator current I and, accordingly, the generator output L_g increases with the increase in N_g along a curve (*abc*) until I reaches 120 A. If the generator has a resistance load and if the allowable maximum current I is limited to 100 A, for example, I will increase along a curve (*ab*) and then along a straight line (*bd*) as shown in Fig. 11.

To simplify the calculation, we assume that E=28-V and $\eta_g \fallingdotseq 0.73$ (in reality E varies with the charging or discharging of the battery; nor is I so constant as given by (*bd*) in Fig. 11).

The torque required for driving the generator, measured at the turbine shaft, can be calculated with

$$(T_g)_t = 6120 L_g / 2\pi N_t \eta_g = 974 L_g / N_t \eta_g = 0.974 EI / N_t \eta_g \text{ kg·m.} \tag{12}$$

In Fig. 23, the output torque of the air-turbine T_t is shown by solid lines against the turbine speed N_t. The thick solid line represents the driving torque of the generator $(T_g)_t$ corresponding to the output power curve (*abc*) in Fig. 11. The broken lines indicate the driving torque $(T_g)_t$ for several values of I from 10 A to 110 A calculated with eq. (12) assuming that E=28 V and η_g=0.73. According to eq. (12), the broken lines should be orthogonal hyperbolas. The chain line indicates the torque corresponding to the maximum output power $(L_t)_{max}$ shown in Fig. 16. If C_z and I are given, and if the solid straight line for C_z touches the broken line for I tangentially, then this point of contact gives the optimum running condition for the system. At this point,

$$T_t = (T_g)_t \tag{13}$$

and

$$\partial T_t / \partial N_t = \partial (T_g)_t / \partial N_t. \tag{14}$$

Now we have from eq. (2)

$$\partial T_t / \partial N_t = -b, \tag{15}$$

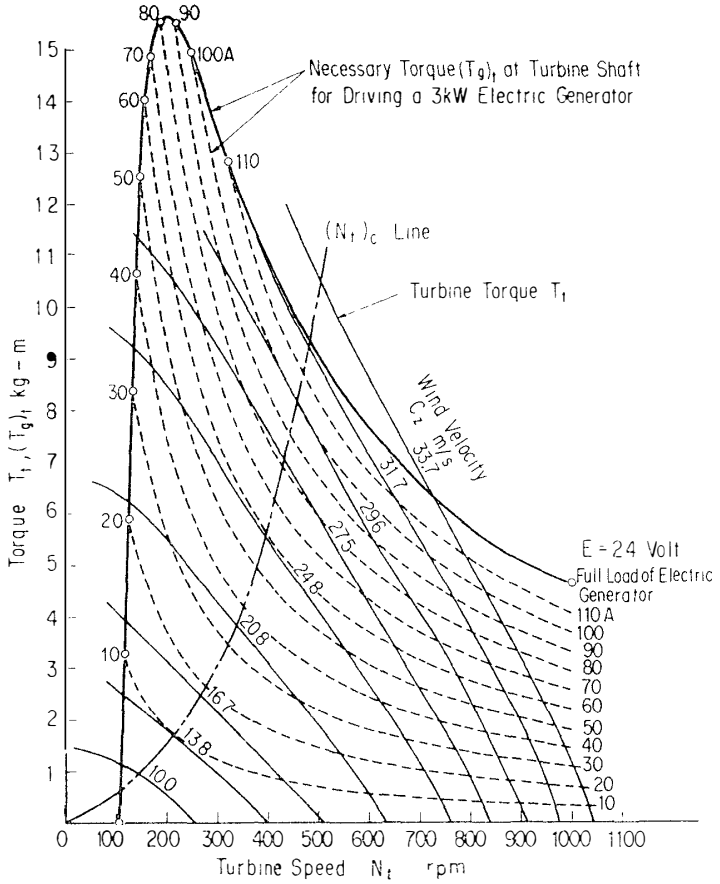

Fig. 23. Torque matching diagram for the NU-102.
Turbine torque T_t vs. turbine speed N_t for various wind velocities (solid lines). $(T_g)_t$ shows the generator input torque at turbine shaft for various loads (broken lines).

and from eq. (12)

$$\partial(T_g)_t/\partial N_t = -0.974EI/N_t^2\eta_g. \tag{16}$$

Substituting eqs. (15) and (16) into eq. (14), we get

$$N_t = \sqrt{0.974EI/b\eta_g} \quad \text{rpm}. \tag{17}$$

For the NU-102,

$$N_t = 40\sqrt{EI/C_z\eta_g} \quad \text{rpm}. \tag{17'}$$

If the straight line T_t for a given wind velocity C_z intersects the broken line for a load current I at two points, the equilibrium turbine speed should satisfy the following equation, which is derived from eqs. (2), (13) and (12);

$$bN_t^2 - aN_t + 0.974EI/\eta_g = 0. \tag{18}$$

The solution of eq. (18) is

$$N_t=(a/2b)\pm\sqrt{(a/2b)^2-0.974(EI/b\eta_g)} \tag{19·a}$$

$$=(N_t)_c\pm\sqrt{(N_t)_c^2-0.974(EI/b\eta_g)} \tag{19·b}$$

where $(N_t)_c$ is the optimum turbine speed giving the maximum power output, which is defined by eq. (7). Eqs. (17) and (19) show that the turbine speed N_t defined by eq. (17) should be equal to the optimum turbine speed $(N_t)_c$ defined by eq. (7).

If the turbine torque is given by eq. (2), the optimum wind velocity $(C_z)_c$ for the optimum turbine speed $(N_t)_c$, which is one half of the maximum turbine speed $(N_t)_{max}$, can be calculated from eqs. (3) and (17):

$$(C_z)_c=2(k_2/k_1)(N_t)_c=(k_2/k_1)(N_t)_{max}\quad \text{m/s} \tag{20}$$

$$=1.573\sqrt[3]{(k_2/k_1^2)(EI/\eta_g)}\quad \text{m/s}. \tag{21}$$

For the NU-102,

$$(C_z)_c=0.0660(N_t)_c=0.0330(N_t)_{max}\quad \text{m/s} \tag{20'}$$

$$=1.906\sqrt[3]{EI/\eta_g}\quad \text{m/s}. \tag{21'}$$

The calculated values of $(N_t)_c$, $(N_t)_{max}$, $(C_z)_c$, the maximum generator output $(L_g)_{max}$, and the maximum turbine output $(L_t)_{max}$ at the optimum state are shown in Table 3 for various load current I. This table shows the relation between the wind velocity C_z and the load current I giving the heighest power of the NU-102.

Table 3. Calculated optimum wind velocity $(C_z)_c$, optimum turbine speed $(N_t)_c$, maximum turbine output power $(L_t)_{max}$, maximum generator output power $(L_g)_{max}$ and maximum turbine speed $(N_t)_{max}$ for various values of load current I of the NU-102 (E= 28 V, η_g=0.73).

Load current I amp.	$(C_z)_c$ m/s	$(N_t)_c$ rpm	$(L_t)_{max}$ kW	$(L_g)_{max}$ kW	$(N_t)_{max}$ rpm
5	11.0	167	0.19	0.14	334
10	13.9	210	0.38	0.28	420
20	17.5	265	0.77	0.56	530
30	20.0	303	1.15	0.84	606
40	22.0	333	1.53	1.12	666
50	23.7	359	1.92	1.40	718
60	25.2	382	2.30	1.68	764
70	26.5	401	2.69	1.96	802
80	27.7	420	3.07	2.24	840
90	28.8	436	3.45	2.52	872
100	29.8	451	3.84	2.80	902
110	30.8	467	4.22	3.08	934
120	31.7	480	4.60	3.36	960

$(C_z)_c=6.43\sqrt[3]{I}$ m/s and $(N_t)_c=15.16(C_z)_c$ rpm for the NU-102.

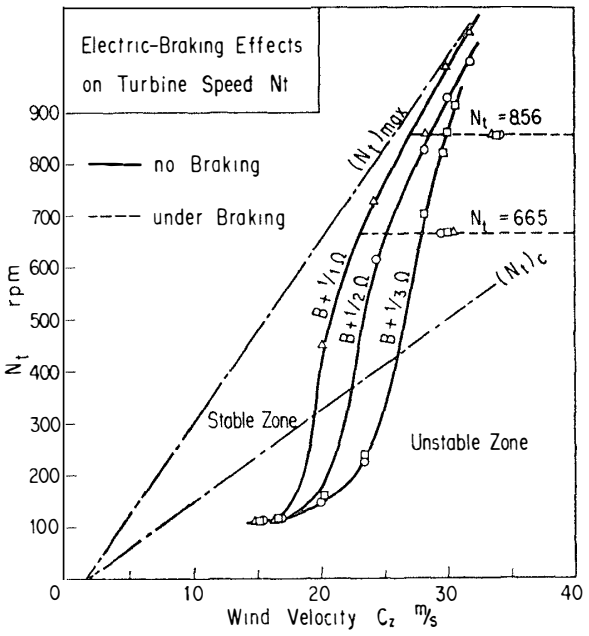

Fig. 24. Stable and unstable zones in N_t vs. C_z relation and the electric braking effect for maintaining a constant turbine speed N_t for any wind velocity.

Generally, there are two equilibrium turbine speeds $(N_t)_L$ and $(N_t)_{II}$ for a pair of values of C_z and I (see eq. (19)). The turbine speed $(N_t)_L$ is lower than the optimum turbine speed $(N_t)_c$ and corresponds to unstable state, because

$$-\partial(T_g)_t/\partial(N_t)_L > -\partial(T_t)/\partial(N_t)_L. \tag{22}$$

The other equilibrium turbine speed $(N_t)_{II}$ corresponds to a stable state, because

$$-\partial(T_g)_t/\partial(N_t)_{II} < -\partial(T_t)/\partial(N_t)_{II}. \tag{23}$$

Fig. 24 shows the variation of N_t with C_z under a constant load for the NU-102. The zone surrounded by the line $(N_t)_{max}$ for no-load and the line $(N_t)_c$ is a stable zone, and the zone below the line $(N_t)_c$ is an unstable zone.

At wind velocities lower than the optimum wind velocity $(C_z)_c$, the turbine rotates with the quasi-equilibrium speed $(N_t)_L$. When the wind velocity increases gradually, the turbine speed jumps up suddenly to a higher equilibrium speed $(N_t)_L$. In the case of the NU-102, $(N_t)_{II}$ in the stable zone approaches the $(N_t)_c$ line at a wind velocity of 26 m/s and for a load $(B+1/3)$, as shown in Fig. 24. Therefore, the highest efficiency can be achieved at this wind velocity under a load of $(B+1/3)$ (Fig. 28).

It is generally desirable that the turbine speed be always kept in the stable zone and increase with the increase in wind velocity along a working line. It is further desirable to keep this working line as close to the $(N_t)_c$ line as possible by controlling the load current I or voltage E automatically.

6. Controlling Turbine Speed by Eddy-Current Brake

The NU-102 has an electric eddy-current brake for governing the turbine speed N_t and, accordingly, the generator speed N_g. By this newly developed means, we can keep the rotational speed at a desired value even with very high wind velocities such as 50–60 m/s, and protect the turbine and generator from over-running.

An electromagnetic pickup is used as a sensor for the generator speed N_g. The small electric current flowing through the magnetizing coil in the brake-stator is controlled automatically so as to maintain a desired generator speed for any wind velocity and load.

The electric eddy-current brake is so designed that it will absorb 35 kW at 3000–6000 rpm with a magnetizing current of about 0.65 A. The broken lines in Figs. 24 and 25 show the turbine speed N_t and the generator output L_g under elec-

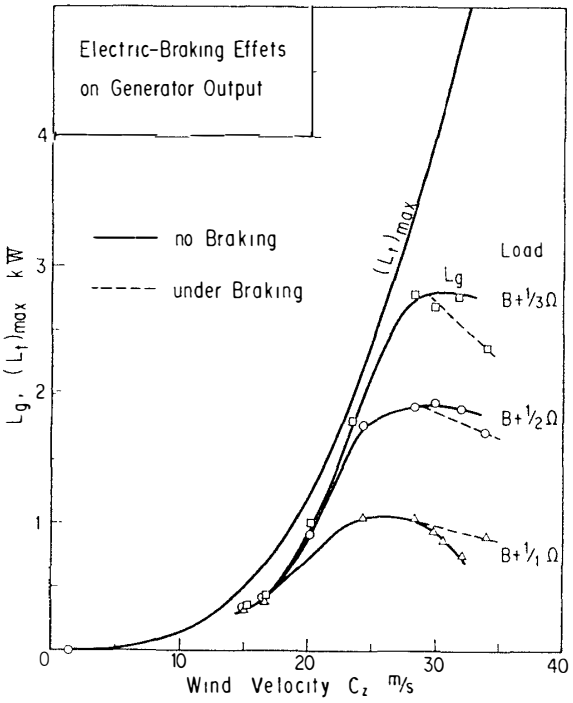

Fig. 25. The effect of the electric braking on the output power of generator L_g at various wind velocities C_z.

tric braking for various wind velocities. These experimental results show that N_g can be kept perfectly constant at a pre-set value but L_g is not.

We have confirmed that this electric eddy-current brake presents a new method for maintaining the maximum speed of an air-turbine within specified limits without any complicated mechanism such as pitch-controlling devices. It is the most economical and effective means for ensuring the safety of the multi-blade air-turbine in violent blizzards. In its operation, part of the turbine output is absorbed by the brake, and the remainder is supplied to the electric generator. As the absorbed energy in the brake is changed into heat and tranferred to the cooling liquid in the jackets, the electric brake can be used also as a heat generator using wind energy.

An experiment to determine the available heat quantity will now be described. A small pump driven by a 140 W electric motor circulates the cooling water between the jackets and a bottom tank shown in Fig. 26. The following quantities and respective symbols are used in the analysis set forth below:

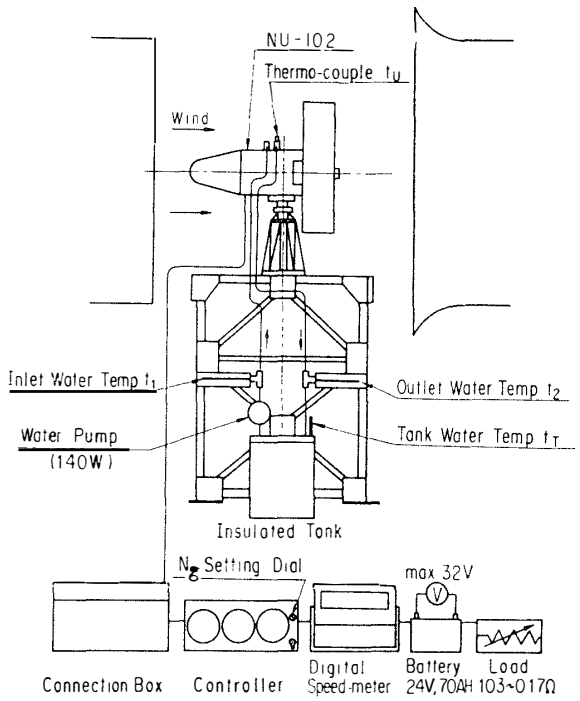

Fig. 26. Experimental equipment for determining heat recovery by braking the NU-102.

Q_H: heat generated in the brake, kcal/h,
Q_c: heat dissipated by the tank and pipes, kcal/h,
t_1: temperature of inlet water to the brake, °C,
t_2: temperature of outlet water from the brake, °C,
t_u: highest water temperature in the jackets, °C,
t_T: water temperature in the tank, °C,

Table 4. Experiments on the heat generated in the eddy-current brake Q_H at a wind velocity $C_z=30$ m/s under various loads ($N_g=4000$ rpm).

No.	Time min	Load	C_z m/s	N_g rpm	E V	I A	L_g kW	Temperature °C				t_u-t_1 °C	t_2-t_1 °C	Q_H kcal/h	Q_C kcal/h	$(L_g/\eta_g)+L_H$ kW
								t_1	t_2	t_u	t_T					
1	5	$B+\frac{1}{6}$	30.2	4004	15.7	84	1.32	45.3	47.5	48.0	45.9	2.7	2.2	2400	1950	4.6
2	10	$B+\frac{1}{5}$	30.0	4004	22.0	72	1.58	50.4	52.1	53.0	50.8	2.6	1.7	2310	1510	4.9
3	12.5	$B+\frac{1}{4}$	30.0	3998	24.5	87	2.13	52.4	53.3	54.0	52.8	1.6	0.9	1410	800	4.6
4	15	$B+\frac{1}{3}$	30.1	3991	28.1	90	2.52	52.5	52.7	54.0	52.9	1.5	0.2	1330	180	5.0
5	18.7	$B+\frac{1}{2}$	30.0	3996	28.1	63	1.77	52.3	53.5	54.0	52.9	1.7	1.2	1510	1070	4.2
6	25.2	$B+\frac{1}{1}$	30.1	3998	28.5	37.5	1.07	57.2	59.0	60.0	58.0	2.8	1.8	2480	1600	4.3

G_w: flow rate of water, 888 kg/h.

The temperature t_1, t_2 and t_T were measured by mercury thermometers; t_u was measured by a thermo-couple and indicated on a temperature gage of the controller. Q_H and Q_e were calculated with following approximate equations:

$$Q_H = G_w(t_u - t_1) \quad \text{kcal/h}, \tag{26}$$

$$Q_e = G_w(t_2 - t_1) \quad \text{kcal/h}. \tag{27}$$

Table 4 shows the experimental results for various load currents under a constant wind velocity of 30 m/s. The generator speed N_g can always be kept within 4000 ± 10 rpm. Q_H varies with the load current I, accordingly with the generator output L_g. The heat Q_H increases from 1300 to 2500 kcal/h with the decrease in L_g. The sum of the generator input L_g/η_g and the equivalent power L_H, calculated as $L_H = Q_H/860$, is 4.6 ± 0.4 kW, which is nearly equal to the maximum turbine output $(L_t)_{max}$ for the wind velocity 30 m/s (see Fig. 25). If Q_H is to be given off to a free air stream with temperature t_z, a radiator having the total surface area A will be required:

$$A = Q_H/K(t_u - t_z) \qquad \text{m}^2. \tag{28}$$

Here K is the over-all coefficient of heat transmission from the cooling liquid to the air, represented in kcal/m^{2}h°C. This value depends on the wind velocity and will be nearly equal to 10–15 kcal/m^{2}h°C for wind velocities around 30 m/s. The necessary surface area will be as great as 2–4 m^2, but in reality, the heat capacity of the liquid reserved in the tank and jackets will assist in decreasing the surface area.

If the eddy-current brake alone is coupled to the output shaft of the air-turbine, all the output can be changed into heat. In case the turbine output is L_t,

$$Q_H = 860 L_t \quad \text{kcal/h}. \tag{29}$$

Table 1 gives the maximum heat output of the NU-102. In Fig. 16 is given the turbine output of the NU-102 obtained by the dynamometer tests. From this figure we may calculate with eq. (29) the heat Q_H that can be obtained by braking. This heat can be utilized for many purposes by circulating the heated liquid through a small pump driven by the air-turbine, or by another small electric motor. For this, the outer surfaces of the brake-stator and pipes should be thermally insulated.

7. Efficiencies of Wind Air-Turbine

7. 1. Total-to-total efficiency and total-to-static efficiency

The following two efficiencies are defined for the wind air-turbine (AWANO *et al.*, 1976) after HORLOCK (1966):

$$\text{total-to-total efficiency} \quad \eta_{TT}=102L_{ti}/[G(C_z^2-C_2^2)/2g], \tag{30}$$

$$\text{total-to-static efficiency} \quad \eta_{TS}=102L_{ti}/[GC_z^2/2g]. \tag{31}$$

Here L_{ti} is the indicated output power of the air-turbine in kW and C_z and C_2 are wind velocity and the residual absolute velocity at the exit of the rotor in m/s, respectively.

The total-to-total efficiency η_{TT} denotes the ratio of the indicated turbine output to the difference of the kinetic energies of the inlet and outlet air stream. It is determined by the aerodynamical losses in the stator and the rotor. The total-to-static efficiency η_{TS} is the ratio of the indicated turbine output to the kinetic energy of the inlet wind. It includes the effect of the leaving loss and the aerodynamical losses. For comparing the performance of wind air-turbines, η_{TS} is more significant than η_{TT}.

From eqs. (30) and (31), we get

$$\eta_{TS}=\eta_{TT}[1-(C_2/C_z)^2]. \tag{32}$$

Obviously, η_{TS} is smaller than η_{TT} because the residual absolute velocity C_2 is smaller than the inlet wind velocity C_z.

From eqs. (30) and (31), the indicated turbine output can be represented by

$$L_{ti}=\eta_{TT}G(C_z^2-C_2^2)/2000=\eta_{TS}GC_z^2/2000 \quad \text{kW}. \tag{33}$$

If the residual absolute velocity C_2 is directed axially and is equal to the mean axial velocity C_{zm} along any radius, eq. (33) can be rewritten as

$$L_{ti}=\eta_{TT}\gamma aC_{zm}(C_z^2-C_{zm}^2)/2000 \quad \text{kW}. \tag{34}$$

From eq. (34), it derives that the following mean axial velocity maximizes L_{ti} (AWANO *et al.*, 1976).

$$C_{xm}=C_z/\sqrt{3} \quad \text{m/s.} \tag{35}$$

The maximum indicated output for this axial velocity is

$$L_{ti,max}=\eta_{TT}\gamma aC_z^3/(3000\sqrt{3}) \quad \text{kW.} \tag{36}$$

From eq. (32), we get

$$\eta_{TS}=(2/3)\eta_{TI} \tag{37}$$

for the axial velocity.

7. 2. Starting wind velocity and friction torque

The minimum wind velocity $(C_z)_0$ required for starting a windmill depends greatly on the friction torque and on the inertia torque of the rotating parts, the former depending mainly on the viscosity of the lubricant. In the NU-102, a very low viscosity lubricant prepared for Antarctica is used, whereby the starting wind velocity is only 1.4–2.0 m/s.

When the turbine speed reaches 100 rpm at a wind velocity of 10.3 m/s, the electric generator begins to generate electric voltage. The starting torque $(T_i)_0$ for a starting wind velocity $(C_z)_0$ may be calculated theoretically with the following equation (AWANO *et al.*, 1976).

$$(T_i)_0=T_f+I_p(d\omega/dt)=\gamma a(C_z)_0^2(\tan\alpha_{1m}+\tan\alpha_{2m})r_m/3g. \tag{38}$$

Here I_p is the polar mass moment of inertia of the rotating parts and ω is the angular speed. Substituting $\alpha_{1m}=39.9°$, $\alpha_{2m}=0°$, and $r_m=0.400$ m and $(C_z)_0=1.4$–2.0 m/s into this equation, we get

$$(T_i)_0=0.027\text{–}0.055 \text{ kg·m.}$$

The friction torque T_f required for starting the rotation is measured experimentally by putting a small weight at the tip of the moving blade. The friction torque T_f of the NU-102 including the air-turbine, speed-up gear, and brake bearing but excluding the generator, was about 0.026–0.06 kg·m, and that including the generator was about 0.06–0.09 kg·m (see Table 5).

The polar mass moment of inertia of the NU-102 was also measured experimentally by the torsional pendulum method (see Table 6). The results indicate

Table 5. Friction torque T_f of the NU-102 measured experimentally.

Direction or rotation	Friction torque T_f kg-m	Remarks
Normal	0.03–0.06	Without generator
	0.07–0.09	With generator
Reversed	0.026	Without generator
	0.060	With generator

Table 6. Polar mass moment of inertia I_p of the NU-102.

Item	I_p kg·cm·s²
Turbine rotor, shaft and planetary gear disk	42.2
Brake-rotor and coupling	1.0
Generator-rotor	0.4
Total sum	43.6 kg·cm·s²

that the friction torque of the NU-102 is approximately 0.06 kg·m, which is negligible compared to the output torque except for very low wind velocities.

7. 3. Theoretical brake output and torque of the air-turbine

In the designed state of the NU-102, the maximum indicated turbine output power is $L_{ti}^*=1.00$ kW (see eq. (36)) if the wind velocity C_z^* is 17 m/s; the theoretical indicated turbine torque is

$$(T_{ti})_{th}^*=6120(L_{ti})_{max}^*/2\pi N_t=6120\times 1.00/2\pi\times 260=3.76 \text{ kg·m}.$$

The theoretical brake turbine torque is

$$(T_{te})_{th}^*=(T_{ti})_{th}^*-T_f=3.70 \text{ kg·m}.$$

The theoretical brake turbine output power for this torque becomes

$$(L_{te,max})_{th}^*=2\pi N_t{}^*(T_{te})_{th}^*/6120=0.989 \text{ kW}.$$

In an off-designed state, the turbine speed N_t increases in proportion to $C_z-(C_z)_0$. Hence, the theoretical turbine speed for any wind velocity C_z will be given by

$$(N_t)_{th}=N_t^*[C_z-(C_z)_0]/[C_z^*-(C_z)_0] \quad \text{rpm}. \tag{39}$$

For the NU-102,

$$(N_t)_{th}=260(C_z-1.4)/(17-1.4)=16.67(C_z-1.4) \quad \text{rpm}. \tag{39'}$$

The theoretical brake torque of an air-turbine for any wind velocity C_z can be estimated by

$$(T_{te})_{th}=\frac{60\gamma a\eta_{TT}C_z^3}{2\pi(N_t)_{th}\sqrt[3]{3}g}-T_f \quad \text{kg·m}. \tag{40}$$

For the NU-120,

$$(T_{te})_{th}=[0.1989C_z^3/(N_t)_{th}]-0.06 \quad \text{kg·m} \tag{40'}$$

and the theoretical brake output power is calculated as

$$(L_{te})_{th}=2\pi(N_t)_{th}(T_{te})_{th}/6120 \quad \text{kW}. \tag{41}$$

The calculated value of $(N_t)_{th}$ and $(L_{te})_{th}$ are compared with the dynamometer and

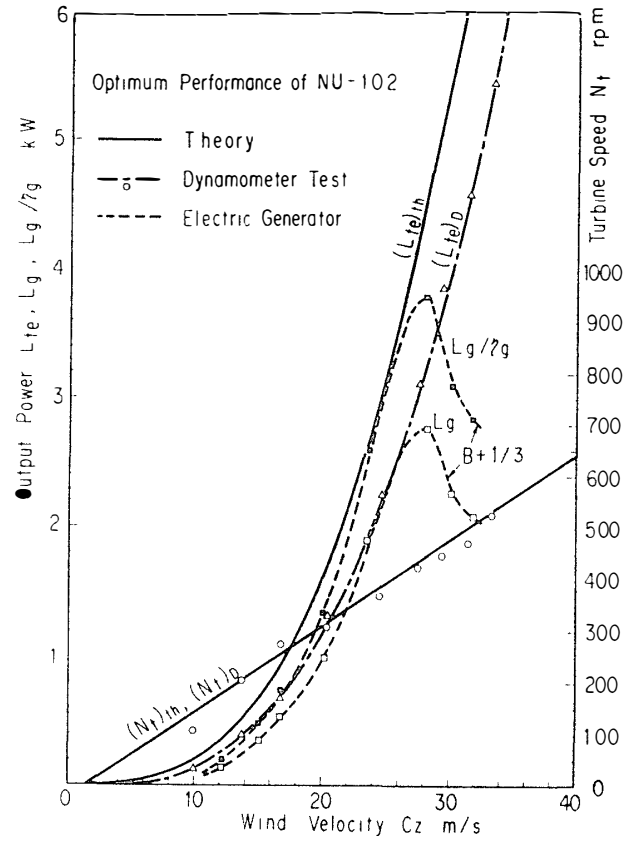

Fig. 27. Comparison of the theoretically calculated turbine output $(L_{te})_{th}$, the best turbine output $(L_{te})_D$ measured by dynamometer, the best actual output of generator L_g and the best actual input of generator L_g/η_g under various wind velocities. The straight line shows that the theoretically determined turbine-speed $(N_t)_{th}$ coincides well with the measured turbine-speeds in the dynamometer test.

generator test results in Fig. 27.

The turbine speed $(N_t)_{th}$ calculated with eq. (39′) agrees with the dynamometer test results $(N_t)_D$ but not with the generator test results, because of the dismatching of the generator to turbine.

On the other hand, the brake output power $(L_{te})_D$ at nominal speed $(N_t)_c$ measured by the dynamometer is only 73–76 % of the theoretical output $(L_{te})_{th}$, which is equal to the percentage of the annulus area that was not shaded by the dymamometer and its bed. This means that the air flow rate G in the dynamometer tests was about 75 % of the designed value.

In Fig. 27, the maximum generator output L_g and the input L_g/η_g under a load $(B+1/3)$ are compared with $(L_{te})_{th}$, assuming that η_g was 73 %. Theoretically, L_g/η_g should be equal to $(L_{te})_{th}$; actually, L_g/η_g is smaller than $(L_{te})_{th}$ for all wind velocities except 24–26 m/s, for which the former approaches the latter. This is

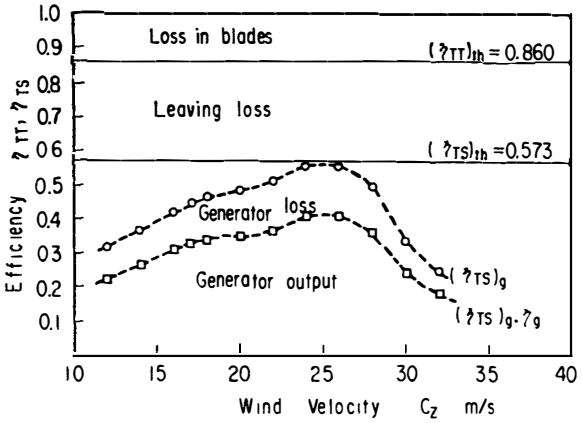

Fig. 28. Total-to-total efficiency η_{TT}, total-to-static efficiency η_{TS}, which are calculated theoretically, and the experimentally obtained $(\eta_{TS})_g$ and $(\eta_{TS})_g\cdot\eta_g$.

because turbine speed in the generator test approaches the designed turbine speed $(N_t)_{th}$, which is equal to the optimum turbine speed $(N_t)_c$ defined by eq. (7), only at 24–26 m/s, as is seen in Fig. 24. At lower wind velocities, the true turbine speed N_t is lower than $(N_t)_c$. At higher wind velocities, N_t is higher than $(N_t)_c$. To neither cases, the designed velocity triangles, Fig. A-1, are applicable, because they are off-design state in their flow directions through the moving blades.

In Fig. 28, the total-to-total efficiency $(\eta_{TT})_{th}$ and the total-to-static efficiency $(\eta_{TS})_{th}$ calculated theoretically are given against the wind velocity. Theoretically, both should be independent of the wind velocity. In the same figure is shown another total-to-static efficiency, in which L_{ti} is replaced by the generator input L_g/η_g, as follows:

$$(\eta_{TS})_g=102(L_g/\eta_g)/(GC_z^2/2g). \tag{42}$$

The following product is also shown in the same figure:

$$(\eta_{TS})_g\eta_g=102L_g/(GC_z^2/2g). \tag{43}$$

Fig. 28 shows that the NU-102 can convert about 57% of the wind energy into mechanical work, and about 42% of the wind energy into electric energy. The latter percentage can be further improved by increasing the generator efficiency. The remaining 43% of the wind energy is dissipated as aerodynamical losses, including the leaving loss that reaches about 30% of the wind energy. This is unavoidable for maintaining a large air flow rate G.

From these experiments it is concluded that what is most important is to develop an electric generator of good efficiency and good matching performance with respect to the coupled air-turbine. It is also desirable to develop automatic load-controlling systems by virtue of which the turbine speed can always be kept slightly higher than and as near as possible to the optimum turbine speed $(N_t)_c$.

8. Theoretical Analysis of the Indicated Turbine-Torque

It has been found in dynamometer tests that the turbine torque T_t can be represented by eqs. (2) and (3). These relations can be verified theoretically as shown below.

Fig. 4 shows an example of the velocity triangles for an air-turbine having a stator. Theoretically, the air flows into the moving blades with an inlet absolute velocity C_1 and leave them with an exit absolute velocity C_2 and the tangential components of C_1 and C_2 are represented by C_{y1} and C_{y2}, respectively. But in the real flow, both of the exit gas angles leaving from the stator and rotor are a little smaller than the designed α_1 and β_2, accordingly the tangential velocities are represented by $\phi_1 C_{y1}$ and $\phi_2 C_{y2}$, where the correction coefficients ϕ_1 and ϕ_2 are a little smaller than 1.

The axial velocity in the real flow can be represented by $\phi_x C_x$, where ϕ_x is another correction coefficient for C_x.

The effective flowing area of the element can be represented by $2\pi\phi_0 r dr$, where ϕ_0 is a coefficient which depends on the percentage of the annulus area that is not shaded by the supports, dynamometer and others.

Then, the infinitesimal torque dT_{ti} acting on a blade element ($2\pi r dr$) at a radius r may on the angular momentum theory be represented as follows:

$$\begin{aligned} dT_{ti} &= 2\pi\phi_0 \frac{\gamma}{g}\phi_x C_x(\phi_1 C_{y1}+\phi_2 C_{y2})r^2 dr \\ &= 2\pi\phi_0 \frac{\gamma}{g}\phi_x C_x^2(\phi_1 \tan\alpha_1+\phi_2 \tan\alpha_2)r^2 dr \\ &= 2\pi\phi_0 \frac{\gamma}{g}\phi_x\phi_1 C_x^2\left(\tan\alpha_1+\frac{\phi_2}{\phi_1}\tan\alpha_2\right)r^2 dr. \end{aligned}$$

By putting $\Phi_1=\phi_0\phi_x\phi_1$ and $\Phi_2=\phi_2/\phi_1$, we obtain

$$\begin{aligned} dT_{ti} &= 2\pi\Phi_1 \frac{\gamma}{g} C_x^2(\tan\alpha_1+\Phi_2 \tan\alpha_2)r^2 dr \\ &= 2\pi\Phi_1 \frac{\gamma}{g} C_x^2[\tan\alpha_1+\Phi_2(\tan\beta_2-U/C_x)]r^2 dr. \end{aligned} \tag{44}$$

As stated before, the air-turbine of the NU-102 has been designed on the bases of "constant nozzle angle and axially leaving velocity design": α_1 for any radius of the stationary blades is kept 39.9° theoretically, α_2 for any radius of the moving blades is 0° only for $C_z^*=17$ m/s and $\omega^*=27.3$ rad/s, which corresponds to a turbine speed $N_t^*=260$ rpm.

Under off-designed conditions, β_1 and α_2 vary with C_z, but α_1 and β_2 shown in eq. (44) are independent of the wind velocity. The exit gas angle from the stator, α_1, is independent to the radius, but the exit gas angle relative to the moving blades, β_2, varies as a function of radius r.

For the NU-102, we can put $\tan\alpha_1=\tan 39.9°=0.836$, $\cos\alpha_1=0.767$, $\sin\alpha_1=0.641$, and $\sin^2\alpha_1=0.411$.

The inlet absolute velocity at hub radius of the rotor, C_{1h}, is represented by eq. (A·4) in the Appendix, and the axial velocity C_x at any radius r can be represented by eqs. (A·2) and (A·3) as follows:

$$C_x=C_{xh}(r/r_h)^{-\sin^2\alpha_1}=C_{1h}\cos\alpha_1(r/r_h)^{-\sin^2\alpha_1}$$
$$=\phi_s C_z\cos\alpha_1(r/r_h)^{-\sin^2\alpha_1}. \tag{45}$$

Here ϕ_s is the velocity coefficient of the stationary blades, which is related to the loss coefficient of the stationary blades ξ_s, which is 0.079, hence

$$\phi_s=1/\sqrt{1+\xi_s}=0.962 \tag{46}$$

as the estimated value for the NU-102.

Substituting these values into eq. (45), we obtain

$$C_x=0.962C_z(0.767)(r/0.2)^{-0.411}$$
$$=0.381C_z r^{-0.411} \quad \text{m/s.} \tag{45'}$$

The exit gas angle relative to the moving blades, β_2, is equal to that of the designed condition, where $\alpha_2=0°$ at any radius. Hence

$$\tan\beta_2=\tan\beta_2^*=U^*/C_x^*=r\omega^*/C_x^*$$
$$=(27.3/0.381\times 17)r^{1.411}$$
$$=4.22r^{1.411}. \tag{47}$$

The tangential velocity U at any radius r for a turbine speed N_t can be rewritten to

$$U=r\omega=2\pi N_t r/60. \tag{48}$$

Substituting eqs. (45') (47) and (48) into eq. (44), we have

$$dT_{ti}=\Phi_1[0.0937C_z^2 r^{-0.822}+\Phi_2(0.473C_z^2-0.0308N_tC_z)r^{0.589}]r^2dr$$
$$=\Phi_1[0.0937C_z^2 r^{1.178}+\Phi_2(0.473C_z^2-0.0308N_tC_z)r^{2.589}]dr. \tag{49}$$

$$T_{ti}=\Phi_1[0.0430C_z^2r^{2.178}+\Phi_2(0.1318C_z^2-0.00858N_tC_z)r^{3.589}]_{r_h=0.2}^{r_t=0.6}$$
$$=\Phi_1[(0.0129+0.0207\Phi_2)C_z^2-0.00135\Phi_2C_zN_t] \quad \text{kg·m.} \tag{50}$$

If $\Phi_1=\phi_0\phi_x\phi_1=0.709$ and $\phi_2=\phi_2/\phi_1=0.637$, eq. (50) becomes

$$T_{ti}=0.0185C_z^2-0.00061C_zN_t \quad \text{kg·m.} \tag{51}$$

This equation agrees with the dynamometer test results shown in eqs. (2) and (3). The theoretical brake torque should be less the friction torque T_f, *i.e.*,

$$(T_{te})_{th}=T_{ti}-T_f. \tag{52}$$

The friction torque T_f of the NU-102 is very small, only 0.06 kg·m.

9. Field Test in Antarctica of the NU-102

9. 1. General performance at high wind velocity

The NU-102 wind air-turbine generator was carried to Syowa Station by JARE–19 in February 1978, and it was set near JARE–7 electric generating hut (Fig. 29). One of the authors, TAKEUCHI, a member of JARE–19, observed the performance of the NU-102 in blizzards of 20–40 m/s in October 1978, and sent two charts, Figs. 30 and 34, to Tokyo by telefax. Fig. 30 shows an example of normal running test results: the output voltage E and current I of the generator, cooling liquid

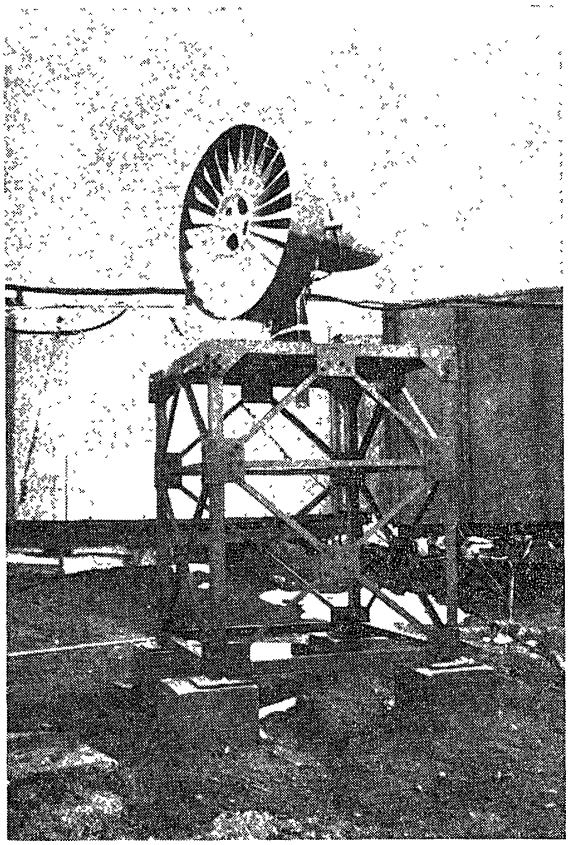

Fig. 29. The NU-102 rebuilt near JARE–7 electric generating hut in February 1978, by JARE–19.

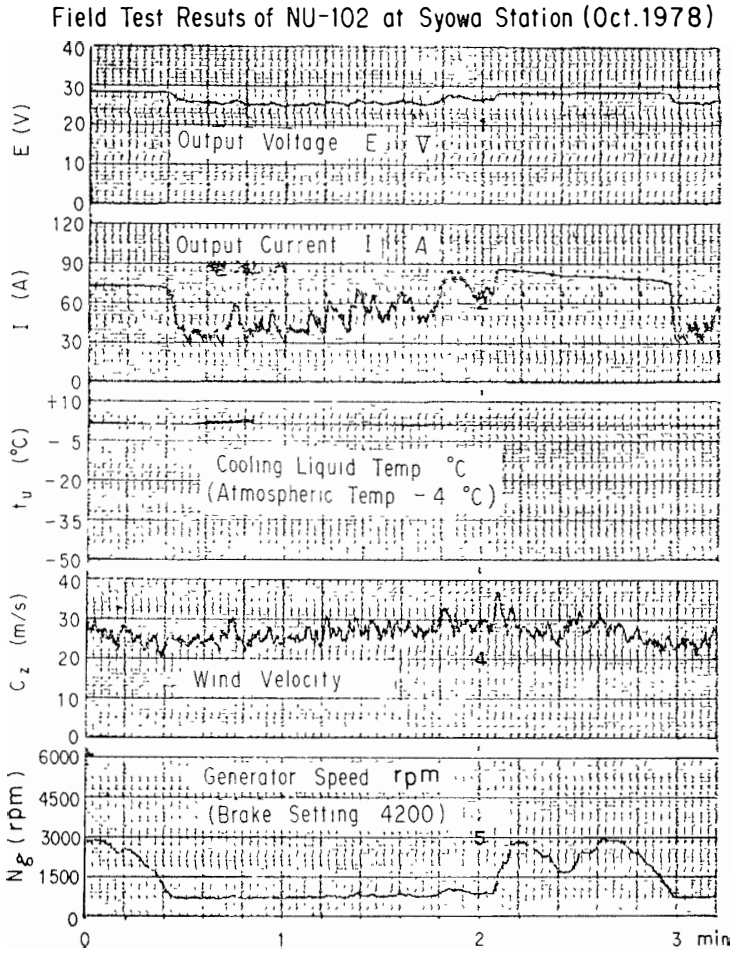

Fig. 30. Results of field tests on the general performance of the NU-102 for high wind velocities at Syowa Station.

temperature t_u of the eddy current brake, wind velocity C_z, and generator speed N_g are given in the chart from top to bottom.

The instantaneous wind velocity was fluctuating between 20 m/s and 37 m/s, being accompanied with changes in the generator speed from 750 rpm to 3000 rpm in three minutes. A 28-V, 120-A battery and a resistance heater were connected in parallel as the load. The internal resistance of the battery in the charging state, the resistance of the heater, and the total resistance of the load are estimated at R_B=4.84 ohms, R_A=0.418 ohms, and R=0.385 ohms, respectively, from the data shown in Fig. 34.

Fig. 30 shows that the generator speed N_g, which is equal to six times the turbine speed N_t, changed with the instantaneous wind velocity with a lag of 12–24 seconds, As shown in Fig. 31, two speed groups, a lower speed group $(N_g)_L$ and a higher speed group $(N_g)_H$, can be observed for one wind velocity. The former,

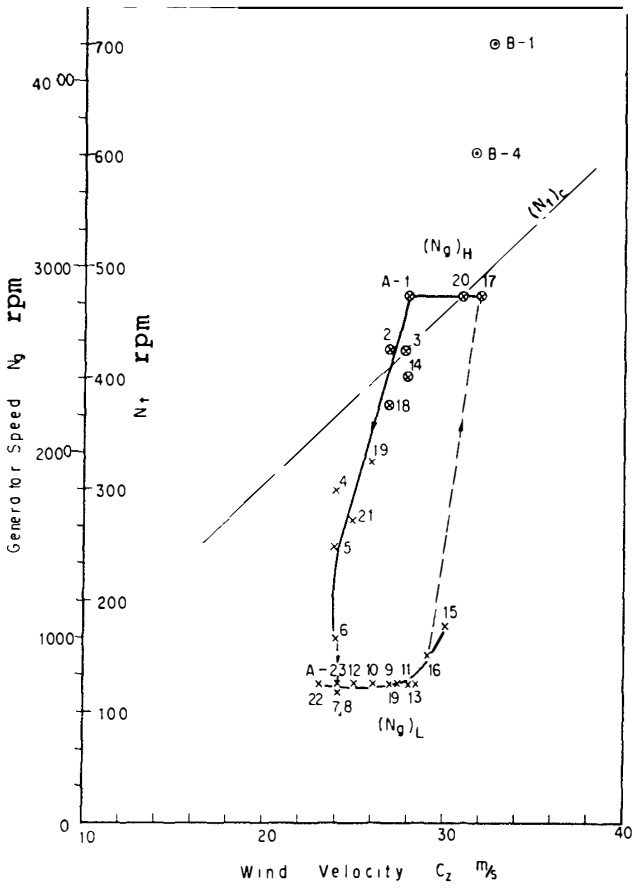

Fig. 31. Instantaneous generator speed for high wind velocities.

$(N_g)_L$ is the quasi-equilibrium generator speed corresponding to the lower turbine speed $(N_t)_L$ in the unstable zone below the nominal turbine speed $(N_t)_c$ (see Section 5 and Fig. 24); $(N_g)_H$ is another equilibrium generator speed corresponding to the higher turbine speed $(N_t)_H$ in the stable zone above $(N_t)_c$.

When the wind velocity exceeds 30 m/s, N_g jumps discontinuously from $(N_g)_L$ group to $(N_g)_H$ group; when it drops below 27 m/s, N_g decreases to $(N_g)_L$ through a transition path and completes a counter-clockwise hysteresis loop.

In Fig. 32 are shown the output voltage E and current I. Each makes a loop when plotted against the wind velocity.

Fig. 33 shows the generator output L_g; the maximum output, 2.38 kW, is obtained at C_z=26–30 m/s.

These results agree with the wind-tunnel test results shown in Figs. 24 and 27 except that the lower speed group of the generator speed $(N_g)_L$ is extended to a higher wind velocity zone than in the wind-tunnel test. The instability is due mainly to the insufficient matching of the generator to air-turbine. It can presumably be avoided by improving the matching of the generator and by the use of

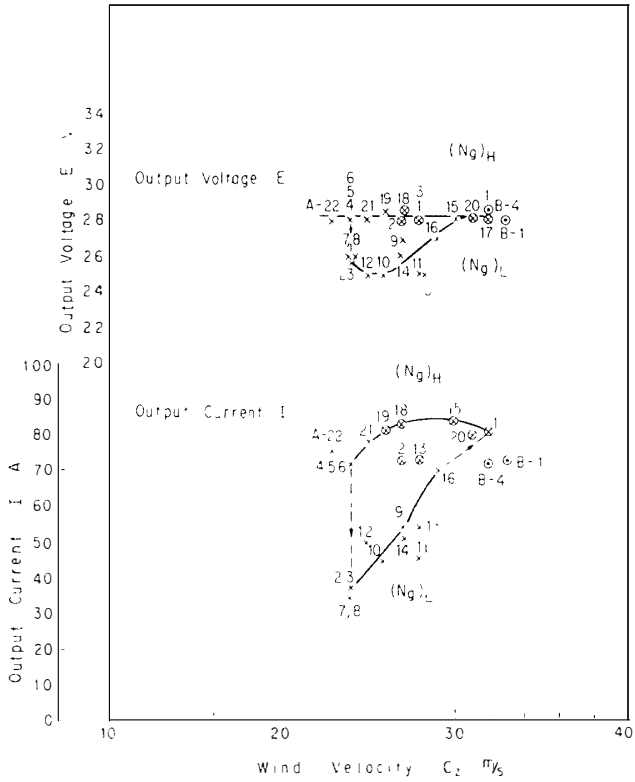

Fig. 32. Output voltages E and output currents I of the NU-102 for high wind velocities.

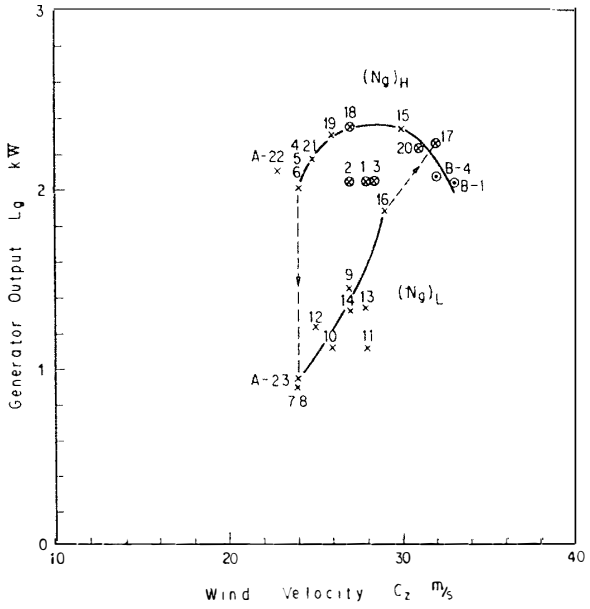

Fig. 33. Generator output L_g of the NU-102 for high wind velocities.

a load controlling system.

9. 2. Electrical braking test

Fig. 34 shows the results of a field test on electrical braking. The maximum generator speed for the wind velocity was pre-set at 4200 rpm. In the first period, a battery (R_B=4.84 ohms) and a resistance heater (R_A=0.418 ohms) were connected to the generator as a load; in the second period the heater was disconnected, and in the third the battery was also disconnected; in the fourth period, both the battery and the heater were again connected.

The N_g chart shows that the generator speed can be kept constant for all the wind velocities and loads met with in these four periods. The points B–1 and B–4 in Figs. 31, 32 and 33 show the values for the first and fourth periods of the experiment.

The temperature curve t_u in Fig. 34 shows the maximum cooling liquid temperature in the jacket of the eddy-current brake. In the first period, the generator

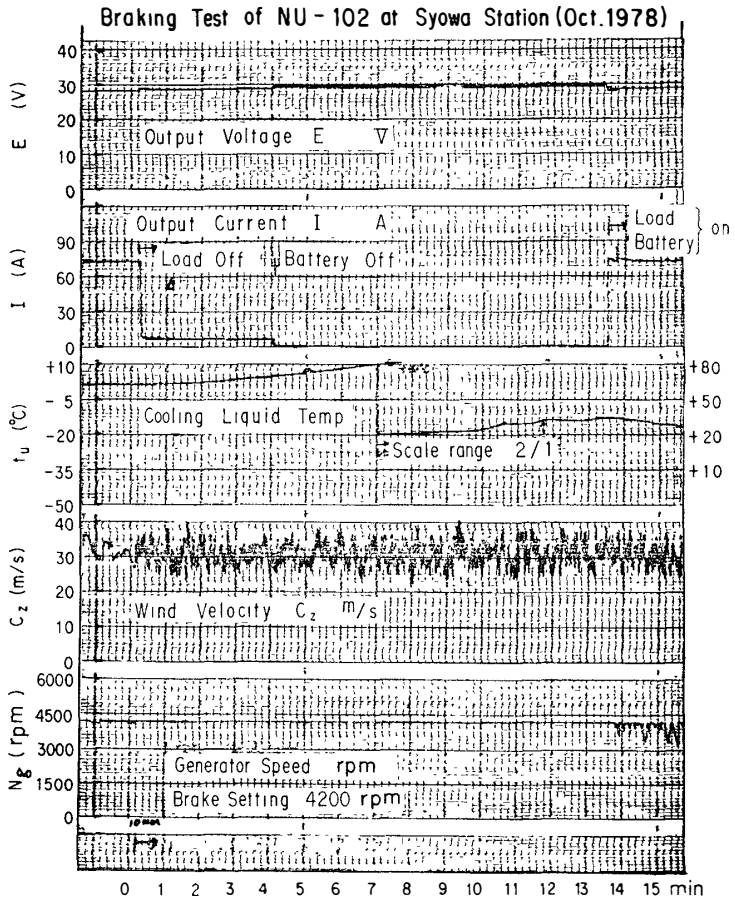

Fig. 34. Results of field tests on the electrical braking of the NU-102 at Syowa Station (October 1978).

output was L_g=2.04 kW (28 V, 73 A) at C_z=33 m/s, and part of the turbine output being absorbed by the electric brake. The atmospheric temperature and the liquid temperature were −4°C and +1°C, respectively.

At the end of the second period, which continued for four minutes, the liquid temperature rose from +1°C to +5°C. In this period, part of the turbine output was absorbed by the generator, and the other part was absorbed by the brake. A power of 0.17 kW (29 V, 6 A) was fed to the battery, so that the power absorbed by the resistance load must been 1.87 kW.

At the end of the third period (no-load, C_z=33 m/s), which continued for 13.3 minutes, the liquid temperature rose from +5°C to 35°C because all of the turbine output was absorbed by the brake.

When the full-load condition was restored again in the fourth period, the liquid temperature was saturated and then gradually decreased because the brake load was light.

These results prove that the electric braking system is very useful.

10. Conclusions

The conclusions of the experimental and theoretical researches on the wind air-turbine electric generator NU-102 are given in the following:

(1) This multi-blade wind air-turbine with a stator gives a higher output power at a lower speed than the ordinary windmill of the same diameter having no stator. The rotational speed of the air-turbine with a stator can be kept much lower than that of the air-turbine without a stator. This results in a lower tensile stress at the root of the moving blades. This is the reason why the present type is suitable for harnessing the high-speed wind energy.

(2) Experiments show that the turbine torque T_t at a wind velocity C_z and for a turbine speed N_t can be represented by $T_t=a-bN_t$, where $a=k_1C_z^2$ and $b=k_2C_z$. The constants k_1 and k_2 are determined by the design. This relation can be derived theoretically by application of the angular momentum theory for turbine torque.

(3) The maximum speed under no-load of the air-turbine for a given C_z is given by $(N_t)_{max}=a/b=(k_1/k_2)C_z$.

(4) The optimum turbine speed giving the maximum output power is half the maximum speed, and is represented by $(N_t)_c=a/2b=(k_1/2k_2)C_z=(N_t)_{max}/2$.

(5) The maximum output power obtained at the optimum turbine speed $(N_t)_c$ is given by $(L_t)_{max}=0.0002568(a^2/b)=0.0002568(k_1^2/k_2)C_z^3$ kW.

(6) The combined performance of the air-turbine and the electric generator depends on the torque matching at the output shaft of the air-turbine. The load current I of the generator should satisfy the following equations which give the optimum turbine speed $(N_t)_c$ and the optimum wind velocity $(C_z)_c$ for obtaining the best output power respectively:

$$(N_t)_c=\sqrt{0.974EI/b\eta_g},$$
$$(C_z)_c=1.573\sqrt[3]{(k_2/k_1^2)(EI/\eta_g)}.$$

Here E and η_g are the output voltage of the generator and the generator efficiency.

(7) The equilibrium of the output torque of the air-turbine and the necessary torque for driving the generator is kept generally at two points. One of which is at a speed $(N_t)_L$ lower than $(N_t)_c$, where the equilibrium is unstable. The speed

will jump up to another value $(N_t)_{II}$ higher than $(N_t)_c$, where the equilibrium is stable. It is desirable that the turbine speed be always in the stable region between the $(N_t)_c$ and $(N_t)_{max}$ lines and as near as possible to the former.

(8) The field test at Syowa Station showed that the maximum generator output L_g was 2.38 kW for wind velocities between 26 and 30 m/s under a total load resistance R=0.385 ohms, in agreement with the wind-tunnel test results. Two values of N_g, E, I and L_g were observed for one wind velocity, one for a higher and the other for a lower generator speed. The former operation condition is stable while the latter is unstable (see (7)). With the changes in wind velocity, the equilibrium state moves along a hysteresis loop in the counter clockwise direction. Such instability will disappear if the matching of the characteristics of the generator and the air-turbine is improved.

(9) The electric eddy-current brake proved to be an effective speed controller for the air-turbine. It can also provide an excellent means for converting the wind energy directly as heat.

(10) The air-turbine NU-102 can convert 57 % of the wind energy to mechanical work, and 42 % of the same to electric energy. The latter percentage may be further improved by increasing the generator efficiency and improving the matching of the generator with the air-turbine.

(11) The direction stabilizing due to its construction of the NU-102, which has no tail, is very effective. Some care should be taken in the design, however, to minimize the area shaded by the supporting stand, nacelle and other parts.

(12) The slip-ring can be omitted if the two cables connecting the elect-generator to the battery are placed loosely around the supporting stand.

Acknowledgment

The authors would like to thank the member of JARE–19 for their cooperation in the test runs at Syowa Station, and Messrs. T. TSURUYA, T. NAKAJIMA and F. MAEDA, graduate students and Messrs. Y. IKEUMI and H. SHINODA, under-graduate students of the Mechanical Engineering Department, as well as the staff of the workshop of Nihon University, for their cooperation in the design, construction and wind-tunnel test of the NU-102. The authors also thank the Toyo Seimitsu Zoki Co., Ltd. for their aid in the construction of the planetary speed-up gear, and are also deeply grateful for the finantial aid rendered by the Ministry of Education (government grant-in-aid for the scientific research and testing No. 285047, 1977) and by the National Institute of Polar Research, Japan.

References

AWANO, S., MURAYAMA, M and TAKEUCHI, S. (1976): Wind electric generator NU-101 driven by

axial-flow air-turbine with stator. Mem. Natl Inst. Polar Res., Ser. F (Logistics) **2**, 47 p.
HORLOCK, J. H. (1966) Axial Flow Turbine. London, Butterworth, 275 p.

(*Manuscript received December 15, 1978; Revised manuscript received May 31, 1979*)

Errata

Memoirs of National Institute of Polar Research,
Series F (Logistics), No. 2, July 1976

AWANO, S. *et al.*: Wind Electric Generator NU-101 Driven by Axial-Flow Air-Turbine with Stator. 47 p.

Eq. (73) in p. 21 should read

$$\nu=(0.138+0.0009t)\times 10^{-4} \quad \mathrm{m^2/s}.$$

The fifth and sixth lines from top in p. 45 should read

$\nu=0.128\times 10^{-4}\mathrm{m^2/s}$ for $t=-10.7°\mathrm{C}$ (at Syowa)
$\nu=0.152\times 10^{-4}\mathrm{m^2/s}$ for $t=15°\mathrm{C}$ (at Tokyo).

APPENDIX

1. Design Data of the NU-102

1.1. Dimensions

External diameter of the outer ring of stator	1.226 m
External diameter of the rotor	1.200 m
Total axial length	1.348 m
Total height	1.473 m
Total weight	346 kg

1.2. Mutiblades wind air-turbine

(a) Stator

Tip radius	$r_t=0.600$ m
Mean radius	$r_m=0.400$ m
Hub radius	$r_h=0.200$ m
Annulus area	$a=1.005$ m^2
Number of stationary blades	$Z_s=45$
Axial chord length	$b=0.135$ m
Chord length	$l=0.163$ m
Spacing at tip radius	$S_t=0.084$ m
at mean radius	$S_m=0.056$ m
at hub radius	$S_h=0.028$ m
Blade design	constant nozzle angle design
Inlet gas angle	$\alpha_0=0°$ for any radius
Outlet gas angle	$\alpha_1=39.9°$ for any radius
Inlet blade angle	$\alpha_0'=0°$ for any radius
Outlet blade angle	$\alpha_1'=41.6°$ for any radius
Stagger angle	$\gamma=34°$
Blade thickness	$t=1.5$ mm
Blade material	SUS 304

The number of the stationary blades was 30 at first, but it was increased to 45 as the output power due to the latter was about 4.9 % greater than that due to the former.

(b) Rotor

Tip radius $r_t=0.600$ m

Mean radius $r_m=0.400$ m

Hub radius $r_h=0.200$ m

Number of the moving blades $Z_R=24$

Blade design Axially leaving velocity, *i.e.*, the exit absolute velocity C_2 from the rotor is directed axially at any radius in the basic design condition. The details of the design are shown in Table A-1.

Table A-1. Design data of the rotor of the NU-102.

Item	$r_h=0.2$ m	$r_m=0.4$ m	$r_t=0.6$ m
Spacing S mm	52	105	157
Chord length l mm	117	117	117
Stagger angle γ deg.	12°	36°	60°
Inlet blade angle β_1' deg.	22.7°	15.5°	49.0°
Outlet blade angle β_2' deg.	25.8°	50.4°	64.4°
Camber angle θ deg.	48.5°	34.9°	15.4°
Inlet gas angle β_1 deg.	22.7°	15.5°	49.0°
Outlet gas angle β_2 deg.	22.7°	48.0°	63.3°
Deflection gas angle ε deg.	45.4°	32.5°	14.3°
Axial velocity C_{xm} m/s	13.0	9.82	8.27
Tangential velocity U m/s	5.45	10.9	16.4
Inlet absolute velocity C_1 m/s	17.0	12.8	10.8
Inlet gas angle for C_1, α_1 deg.	39.9°	39.9°	39.9°
Outlet gas angle for C_2, α_2 deg.	0°	0°	0°

The wind velocity for the basic design $C_z^*=17$ m/s.

2. Velocity triangles of the NU-102 air-turbine

2.1. Stator

The air axially enters the stator at any radius, *i.e*, the inlet gas angle $\alpha_0=0°$. From eq. (35), the mean axial velocity C_{xm} for producing the maximum turbine output is determined for a wind velocity $C_z=17$ m/s as follows:

$$C_{xm}=C_z/\sqrt{3}=17/\sqrt{3}=9.82 \text{ m/s},$$

$$C_0=9.82 \text{ m/s}, \quad \alpha_0=0°.$$

The stator is designed on the basis of the "constant nozzle angle design", *i.e.*, the gas angle α_1 from the stator is kept constant for any radius. For this design, the following conditions should be satisfied (AWANO *et al.*, 1976):

$$C_{y1}=K_1 r^{-\sin^2\alpha_1} \tag{A·1}$$

$$C_{x1}=K_1(\cot\alpha_1)r^{-\sin^2\alpha_1} \tag{A·2}$$

$$C_1=K_1(\mathrm{cosec}\,\alpha_1)r^{-\sin^2\alpha_1} \tag{A·3}$$

where K_1 is a constant. These equation show that C_{y1}, C_{x1} and C_1 decrease with increase of radius r.

In this design, the degree of reaction at hub radius is chosen as zero, *i.e.* it is in an impulse stage at the root, and the degree of reaction increases with radius. Hence, the maximum of the velocity C_1 is realized at hub radius r_h, which is denoted by C_{1h}, and it is related to the wind velocity C_z as follows:

$$C_{1h}=\phi_s C_z. \tag{A·4}$$

Here ϕ_s is the velocity coefficient of the stationary blades, which is slightly smaller than and nearly equal to 1. In front of the stator, the velocity is retarded from C_z to C_0 and accelerated again to C_1 in the stator.

From eqs. (A·2) and (A·4)

$$\begin{aligned}(C_{x1})_h&=(C_{x1})_m(r_m/r_h)^{\sin^2\alpha_1}\\&=C_{1h}\cos\alpha_1=\phi_s C_z\cos\alpha_1.\end{aligned}$$

Substituting eq. (35) for $(C_{x1})_m$, we obtain

$$(r_m/r_h)^{\sin^2\alpha_1}=\sqrt{3}\,\phi_s\cos\alpha_1. \tag{A·5}$$

By putting $(r_m/r_h)=2$ for the NU-102 and $\phi_s=1$ approximately, the solution of the following equation gives the exit velocity angle α_1 as 39.9°:

$$2^{\sin^2\alpha_1}=\sqrt{3}\cos\alpha_1. \tag{A·5′}$$

2.2. Rotor

(a) Velocity triangle at hub radius

The axial velocity at the hub radius is

$$C_{xh}=C_{1h}\cos\alpha_1=17.0\times\cos 39.9^\circ=13.0\ \mathrm{m/s}$$

and the tangential velocity at the hub radius is calculated as

$$U_h=(C_{1h}\sin\alpha_1)/2=(17.0\times\sin 39.9^\circ)/2=5.45\ \mathrm{m/s}.$$

Accordingly, the angular velocity and the turbine speed at the design point are

$$\omega^*=U_h/r_h=5.45/0.200=27.3\ \mathrm{rad/s},$$

$$N_t^*=60\omega^*/2\pi=260\ \mathrm{rpm}.$$

As the stage is a pure impulse stage at the hub radius, the following relation sholud be satisfied, when the exit absolute velocity is directed axially:

$$W_{1h}=W_{2h}=\sqrt{C_{xh}^2+U_h^2}=\sqrt{13.0^2+5.45^2}=14.1\ \mathrm{m/s},$$

$$\text{Cos}\,\beta_{1h}=C_{xh}/W_{1h}=13.0/14.1=0.922 \quad \beta_{1h}=22.7°,$$

$$\text{Cos}\,\beta_{2h}=C_{xh}/W_{2h}=13.0/14.1=0.922 \quad \beta_{2h}=22.7°.$$

(b) Velocity triangle at mean radius

From eq. (A·3)

$$C_{1m}=C_{1h}(r_m/r_h)^{-\sin^2\alpha_1}=17.0(0.4/0.2)^{-\sin^2 39.9°}=12.8 \text{ m/s},$$

$$C_{xm}=9.82 \text{ m/s},$$

$$U_m=r_m\omega^*=0.4\times 27.3=10.9 \text{ m/s},$$

$$W_{1m}=\sqrt{C_{1m}^2+U_m^2-2C_{1m}U_m \sin\alpha_1}=10.2 \text{ m/s},$$

$$W_{2m}=\sqrt{C_{xm}^2+U_m^2}=14.7 \text{ m/s},$$

$$\text{Cos}\,\beta_{1m}=C_{xm}/W_{1m}=9.82/10.2=0.963 \quad \beta_{1m}=15.5°,$$

$$\text{Cos}\,\beta_{2m}=C_{xm}/W_{2m}=9.82/14.7=0.670 \quad \beta_{2m}=48.0°.$$

(c) Velocity triangle at tip radius

In the same way as the case of mean radius, the velocities and their angles at the tip of the rotor are given by

$$C_{1t}=C_{1h}(r_t/r_h)^{-\sin^2\alpha_1}=17.0\times(0.6/0.2)^{-\sin^2 39.9°}=10.8 \text{ m/s},$$

$$C_{xt}=C_{xh}(r_t/r_h)^{-\sin^2\alpha_1}=13.0\times(0.6/0.2)^{-\sin^2 39.9°}=8.27 \text{ m/s},$$

$$U_t=r_t\omega^*=0.600\times 27.3=16.4 \text{ m/s},$$

$$W_{1t}=\sqrt{C_{1t}^2+U_t^2-2C_{1t}U_t \sin\alpha_1}=12.6 \text{ m/s},$$

$$W_{2t}=\sqrt{C_{xt}^2+U_t^2}=18.4 \text{ m/s},$$

$$\text{Cos}\,\beta_{1t}=C_{xt}/W_{1t}=8.27/12.6=0.656 \quad \beta_{1t}=49.0°,$$

$$\text{Cos}\,\beta_{2t}=C_{xt}/W_{2t}=8.27/18.4=0.449 \quad \beta_{2t}=63.3°.$$

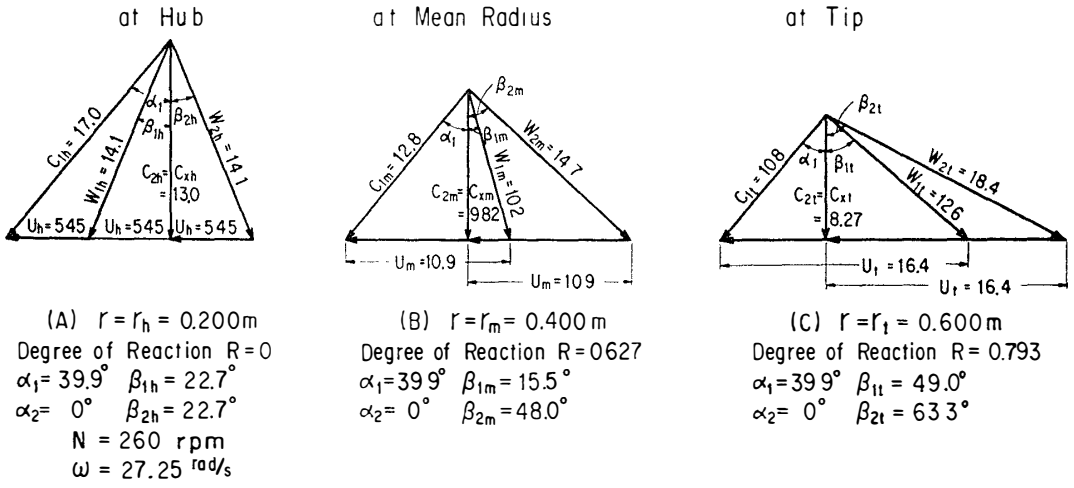

(A) $r=r_h=0.200$m
Degree of Reaction R=0
$\alpha_1=39.9°$ $\beta_{1h}=22.7°$
$\alpha_2=0°$ $\beta_{2h}=22.7°$
N = 260 rpm
$\omega=27.25$ rad/s

(B) $r=r_m=0.400$m
Degree of Reaction R=0627
$\alpha_1=39.9°$ $\beta_{1m}=15.5°$
$\alpha_2=0°$ $\beta_{2m}=48.0°$

(C) $r=r_t=0.600$m
Degree of Reaction R=0.793
$\alpha_1=39.9°$ $\beta_{1t}=49.0°$
$\alpha_2=0°$ $\beta_{2t}=63.3°$

Fig. A-1. Velocity triangles of the NU-102 at the basic design wind belocity $C_z^*=17$ m/s.

The velocity triangles for hub radius, mean radius, and tip radius are shown in Fig. A-1.

3. Estimation of blade angle

As the air-flow enters axially into the stator, the inlet blade angle should be $\alpha_0'=\alpha_0=0°$. But the exit blade angle of the stator is slightly greater than the exit velocity angle α_1, because the air-flow is not deflected perfectly along the blades. The deviation angle δ can be estimated from the experimental data on steam and gas turbine (HORLOCK, 1966). At the mean radius of the stator,

stagger angle $\gamma=34.0°$,
chord length $l=0.163$ m,
spacing $S=0.056$ m

the deviation angle δ is represented by the "constant rule" as

$$\delta=m\theta\sqrt{S/l} \tag{A·6}$$

where m is a constant given for each of the circular and parabolic camber lines as a function of stagger angle γ. In eq. (A·6), θ means the camber angle and is given by

$$\theta=\alpha_0'+\alpha_1' \tag{A·7}$$

for the stator.

For the stator of the NU-102

$$m=0.071 \quad \theta=41.6° \quad \delta_s=1.7°.$$

Hence, the exit blade angle $\alpha_1'=\alpha_1+\delta_s=39.9°+1.7°=41.6°$.

The deviation angles for the moving blade can be estimated in the same way. The results are shown in Table A-2.

Table A-2. Deviation angles and exit blade angles of the moving blade.

Item		$r_h=0.200$ m	$r_m=0.400$ m	$r_t=0.600$ m
Stagger angle	γ	12.0°	36.0°	60.0°
Chord length	l	0.117 m	0.117 m	0.117 m
Spacing	S	0.052 m	0.105 m	0.157 m
Constant	m	0.097	0.074	0.062
Deviation angle	δ_R	3.1°	2.4°	1.1°
Exit gas angle	β_2	22.7°	48.0°	63.3°
Exit blade angle	β_2'	25.8°	50.4°	64.4°

4. Electric generator

For the electric generator of the NU-102 the following AC–DC generator is used, which is a conventional generator for marine diesel engines;

Maker	Sawafuji Denki Co., Ltd., Tokyo	
Type	A 30101 A–24B	
	separately exited type	
	earth floating type (two-lines system)	
	nominal output	3 kW
	rated performance	28 V, 110 A, 3000 rpm
	operating speed range	1000–6000 rpm
	charge starting at	27 V, 900 rpm
	direction of rotation	clockwise as viewed from the driving side
	set regulator	T–30051–24
Size	375(L)×253(H)×170(B) mm	
Weight	35 kg	

The electric circuit diagram is shown in Fig. A-2, and the performance is given in Fig. 11.

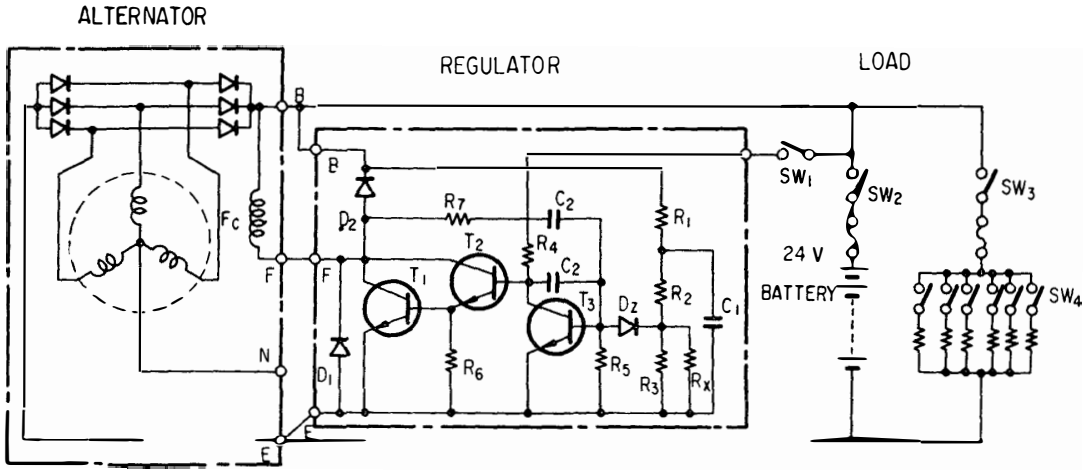

Fig. A-2. The electrical circuit of the Sawafuji 3-kW, AC–DC electric generator.

5. Evaluation of blade losses and turbine efficiencies

The aerodynamical losses in the stationary blades and the moving blades can be estimated theoretically as follows (HORLOCK, 1966; AWANO *et al.*, 1976).

The kinematic viscosity of air is represented by

$$\nu=(0.138+0.0009t)\times 10^{-4} \quad \mathrm{m^2/s} \tag{A·8}$$

where t is the air temperature in °C and for $t=20$°C, $\nu=0.156\times 10^{-4}$ m²/s.

(*a*) *Loss coefficient of stationary blades*

The Reynolds number based on the exit velocity and the hydraulic mean di-

ameter at the throat section of the stationary blades is

$$R_h=[2HS\cos\alpha_1/(S\cos\alpha_1+H)]C_1/\nu, \tag{A·9}$$

$R_h=[2\times0.400\times0.056\times\cos 39.9°/(0.056\times\cos 39.9°+0.400)](12.8)/(0.156\times10^{-4})$
$=6.37\times10^4$.

The loss coefficient of the stationary blades is represented by

$$\xi_s=\left(\frac{10^5}{R_h}\right)^{1/4}\left[(1+\xi_s')\left(0.975+0.075\frac{b}{H}\right)-1\right] \tag{A·10}$$

where

$$\xi_s'=0.062-0.10(\Delta/l)+0.065\times10^{-4}\varepsilon_s^2. \tag{A·11}$$

For the stationary blade of the NU-102

thickness ratio	$\Delta/l=0.009$,
deflection angle	$\varepsilon_s=\alpha_0+\alpha_1=39.9°$,
axial chord	$b=0.135$ m,
blade height	$H=0.400$ m.

Substituting these values into eq. (A·11) and eq. (A·10), we get $\xi_s'=0.071$ and $\xi_s=0.079$.

(*b*) *Loss coefficient of the moving blades*

The Reynolds number based on the exit relative velocity and the hydraulic mean diameter at the throat section of the moving blades is

$$R_h=\left(\frac{2HS\cos\beta_2}{S\cos\beta_2+H}\right)W_2/\nu, \tag{A·12}$$

$$R_h=\left(\frac{2\times0.400\times0.150\times\cos 48°}{0.150\times\cos 48°+0.400}\right)\frac{14.7}{0.156\times10^{-4}}=11.3\times10^4.$$

The loss coefficient of the moving blades is

$$\xi_m=\left(\frac{10^5}{R_h}\right)^{1/4}\left[(1+\xi_m')\left(0.975+0.075\frac{b}{H}\right)-1\right] \tag{A·13}$$

where

$$\xi_m'=0.062-0.010(\Delta/l)+0.065\times10^{-4}\varepsilon_m^2. \tag{A·14}$$

For the moving blades of the NU-102

thickness ratio	$\Delta/l=0.10$,
deflection angle	$\varepsilon_m=\beta_2-\beta_1=33°$,
axial chord	$b=0.094$ m,
blade height	$H=0.400$ m.

Substituting these values into eq. (A·14) and eq. (A·13), we get $\xi_m'=0.059$ and $\xi_m=0.050$.

(*c*) *Total-to-total efficiency and total-to-static efficiency*

The total-to-total efficiency η_{TT} can be calculated theoretically by (AWANO *et al.*, 1976),

$$\eta_{TT}=1/(1+\zeta) \tag{A·15}$$

where

$$\zeta=\frac{\xi_s C_1^2+\xi_m W_2^2}{(C_z^2-C_2^2)-(\xi_s C_1^2+\xi_m W_2^2)}, \tag{A·16}$$

$$=\frac{22.8+10.8}{(17^2-9.82^2)-(0.079\times 17^2+0.050\times 14.7^2)}=0.174.$$

Substituting into eq. (A·15),

$$\eta_{TT}=1/(1+0.174)=0.852.$$

From eq. (37), the total-to-static efficiency η_{TS} is given by

$$\eta_{TS}=(2/3)\eta_{TT}=0.568.$$